DESIGN AND ANALYSIS OF AEROSTATIC BEARINGS OF CRYOGENIC TURBINES FOR HELIUM REFRIGERATOR/LIQUEFIER

Thesis submitted in partial fulfillment of the requirements for the degree of

Master of Technology

In

Mechanical Engineering

(Cryogenic and Vacuum Technology)

By

Dhiren Mohapatra
Roll No. 213ME5450

DEPARTMENT OF MECHANICAL ENGINEERING
NATIONAL INSTITUTE OF TECHNOLOGY ROURKELA

DESIGN AND ANALYSIS OF AEROSTATIC BEARINGS OF CRYOGENIC TURBINES FOR HELIUM REFRIGERATOR/LIQUEFIER

Thesis submitted in partial fulfillment of the requirements for the degree of

Master of Technology

In

Mechanical Engineering

By

Dhiren Mohapatra
Roll No. 213ME5450

Under the guidance of

Mr. A. K. Sahu

Scientist / Engineer – SF
Division Head,
Large Cryogenic Plant and Cryosystem,
Institute for Plasma Research,
Bhat, Gandhinagar-382428
Gujarat

Prof. R. K. Sahoo

Department of Mechanical Engineering,
National Institute of Technology,
Rourkela-769008
Odisha

National Institute of Technology
Rourkela

CERTIFICATE

This is to certify that the thesis entitled, "**Design And Analysis Of Aerostatic Bearings Of Cryogenic Turbines For Helium Refrigerator/Liquefier**" submitted to **National Institute of Technology, Rourkela** by **Dhiren Mohapatra,** Roll No**. 213ME5450** for the award of the Degree of **Master of Technology** in **Mechanical Engineering** with specialization in "**Cryogenic and Vacuum Technology"** is a record of bonafide research work carried out by him under my supervision and guidance. The results presented in this thesis have not been, to the best of my knowledge, submitted to any other University/ Institute for the award of any degree or diploma. The thesis, in my opinion, has reached the standards fulfilling the requirement for the award of degree of **Master of Technology** in accordance with regulations of the Institute.

Mr. A. K. Sahu

Scientist / Engineer – SF
Division Head,
Large Cryogenic Plant and Cryosystem,
Institute for Plasma Research,
Bhat, Gandhinagar-382428
Gujarat

Prof. R.K Sahoo

Department of Mechanical Engineering,
National Institute of Technology
Rourkela-769008
Odisha

CERTIFICATE

This is to certify that the dissertation, entitled

"**Design and Analysis of Aerostatic Bearings of Cryogenic Turbines for Helium Refrigerator/Liquefier**"

Is a bonafide work done by

Dhiren Mohapatra

Under my close guidance and supervision in the Large Cryogenic Plant and Cryosystem Group of

Institute for Plasma Research, Gandhinagar, Gujarat

for the partial fulfillment of the award of the Degree of **Master of Technology** in **Mechanical Engineering** with specialization in **Cryogenic and Vacuum Technology**

at

National Institute of Technology, Rourkela

The work presented here, to the best of my knowledge, has not been submitted to any university for the award of similar degree.

Mr. A. K. Sahu

Scientist / Engineer – SF

Division Head,

Large Cryogenic Plant and Cryosystem,

Institute for Plasma Research,

Bhat, Gandhinagar-382428

Gujarat

ACKNOWLEDGEMENT

I am extremely thankful to ***Mr. A.K. SAHU*** Scientist / Engineer – SF, Division Head, Large Cryogenic Plant and Cryosystem, Institute for Plasma Research, for his erudite suggestions, perceptive remarks, wondrous guidance and affection. I remain ever grateful to him for his valuable suggestions for the accomplishment of this project work.

I take this opportunity to express my profound sense of gratitude and indebtedness to my supervisor ***Prof. R. K. SAHOO***, Professor, Department of Mechanical Engineering, NIT Rourkela, for his encouragement, guidance and great support during the project work. He was always motivated and shares his expertise during the whole course of project work. I owe a deep debt of gratitude to him and remain grateful to him.

I would like to thank my colleagues, working with me at the Institute for Plasma Research for their great support and advices at hard times.

I shall be failing in my duty, if I don't express my thanks to **NIT ROURKELA** for providing me the financial help in the form of stipend and also encouragement to complete the study successfully.

Last but not the least, I want to convey my heartiest gratitude to my parents and friends for their immeasurable love, support and encouragement.

Dhiren Mohapatra
Roll no. 213ME5450
Cryogenic and Vacuum Technology
Mechanical Engineering Department
National Institute of Technology
Rourkela

ABSTRACT

Aerostatic bearings are generally used in the field of high speed applications. The Helium Refrigerator/Liquefier (HRL) needs turbines as expansion machines to produce cooling effect which is further used for production of liquid helium. Cryogenic turbines are significantly smaller in size compared to those for room temperature applications but rotational speed is very high, about few hundred thousands of rpm and hence these have contactless gas bearings or magnetic bearings. This project involves the design and analysis of the aerostatic bearings with horizontal shaft configuration. In the aerostatic bearings, pressurized helium gas is passed through the bearings. Based on this pressure and temperature and the rotational speed of the turbines, the shaft of the turbine rotates without contact with bearing wall and the leakage between process gas and bearing gas is minimum. For different normal and off-normal operations, speeds will be different and hence the flow parameters for bearing gas flow will be controlled via control valves and the bearing should be designed to provide such contactless rotation. In this study, a theoretical analysis is presented for the load capacity, stiffness, flow rate of aerostatic journal bearing and thrust bearing with pocketed orifice. Effects of orifice diameter, radial clearance, inlet pressure and outlet pressure on load capacity, mass flow rate and stiffness have been analyzed. Dynamic unbalances like whirling of the shaft have also been covered in this study. Design considerations for limiting dispersion effect, and to avoid pneumatic hammer has also been taken into account. Validation of the analysis has been done by using ANSYS CFX with the numerical results.

Keywords: *Aerostatic journal bearing, aerostatic thrust bearing, pneumatic hammer, dispersion effect, dynamic unbalance, whirling, load capacity, stiffness, mass flow rate, ANSYS CFX.*

Table of Contents

List of figures

List of Tables

Nomenclature

a	radius of journal bearing
b	pocket depth
C	damping constant
C_d	coefficient of discharge
C_L	load coefficient
C_{Lo}	load coefficient of axial flow model of journal bearing
d_o	diameter of orifice
d_R	pocket diameter
D	diameter of bearing
G	slot factor
h	radial clearance
h_o	radial clearance at no load
I	transverse moment of inertia of the rotor
I_o	polar moment of inertia of the rotor
2J	distance between the bearings
K	stiffness of bearing
K_g	optimum gauge pressure ratio
l	distance of orifice form end of bearing
L	length of journal bearing
L_S	length of shaft
m	mass flow rate through orifice
m_R	mass of rotor
M	bearing mass flow rate
n	no of feed holes per row
N	total no of feed holes
O	centre of the bearing

O’	centre of the rotating shaft
P_a	pressure at the ends of bearing
P_0	supply pressure
P_d	pressure downstream of restrictor
P_t	pressure at the throat of orifice
r	radius of whirling
R	gas constant
R_1	inner diameter of thrust bearing
R_2	outer diameter of thrust bearing
R_3	feedhole ring position of thrust bearing
T	absolute temperature
W	load on bearing
W_s	aerostatic load capacity of journal bearing
W_d	aerodynamic load capacity of journal bearing
X	static unbalance
x	flow width
	rectangular coordinate
Y	dynamic unbalance
y	flow length
	rectangular coordinate
δ_L	inherent compensation factor
$\Lambda_s\xi$	feeding parameter
ξ	shape factor
η	damping constant per unit rotor mass
β	tilt angle of the rotor
ϕ	attitude angle
ϕ_H	hybrid attitude angle

ω	angular velocity of rotor
ω_1	cylindrical synchronous resonance speed
ω_2	conical synchronous resonance speed
ω^*	angular velocity of whirl/vibration
ω_c	onset speed of self excited whirl
γ	ratios of specific heats of gas (C_p/ C_v)
δ	phase angle by which rotor whirl lags unbalance
θ	angle measured from the load line of journal bearing
μ	viscosity

1 INTRODUCTION

1.1 Helium Liquefaction Process at IPR

Large-scale helium refrigeration/liquefaction (HRL) plants are used for cooling superconducting magnets. The liquefaction process diagram of the Indigenous HRL being developed at Institute for Plasma Research (IPR) for tokamak is shown in the Figure 1.1.

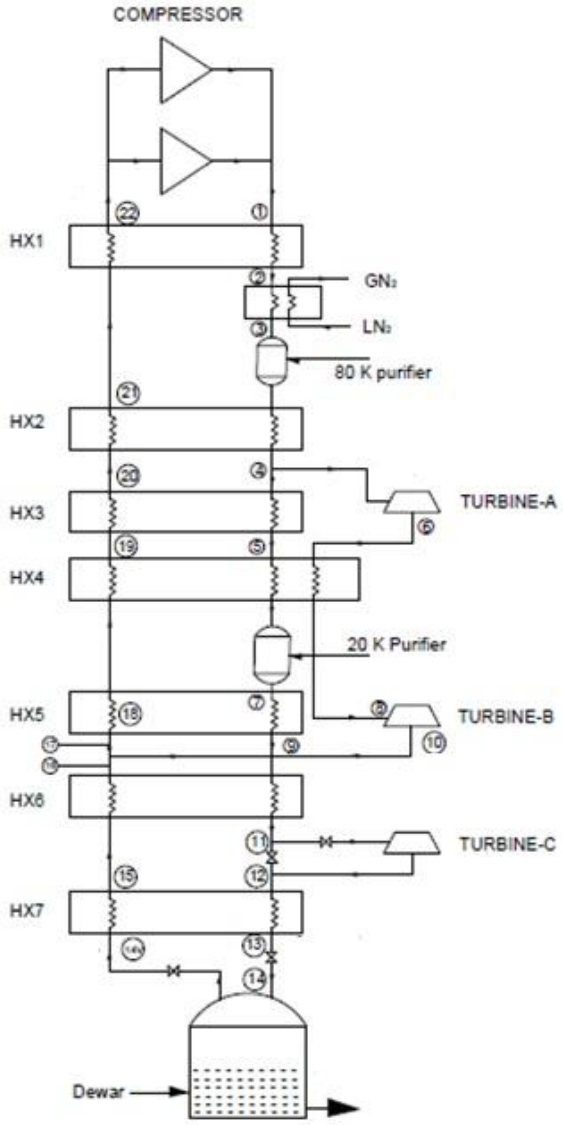

Figure 1.1: Schematic diagram of indigenous HRL plant

Figure 1.1 shows a typical schematic diagram of helium refrigeration and liquefaction plant. Where, present study involves the design and analysis for aerostatic bearings for turbo-expanders.

1.2 Role of Gas Bearing in Cryogenic Application

Cryogenic turbo-expanders are very smaller in size in comparison to those of used in other applications like thermal power plants. The rotational speed is of few hundred thousand

per minute. To support the rotation of turbo-expander, bearings with zero wear and high stiffness is highly required. So for this, generally two cylindrical journal bearings and two thrust bearings are used in combine. But, an alternative method was used in some experiments by using tapered bearing. This tapered bearing acts as the combination of cylindrical journal bearing and thrust bearing. But for this, the geometry of the shaft has to be tapered.

But, recently there is another effective bearing, magnetic bearing, suitable for high speed and very high speed applications.

1.3 Types of gas bearing

There are two types of gas bearings.

- Aerodynamic
- Aerostatic (Also called as Externally pressurized gas bearing)

1.3.1 Aerodynamic bearing

In aerodynamic bearing, the relative motion between the two surfaces generates the pressure differential, which helps the shaft to float on the gas layer. There are different kinds of aerodynamic bearings. No pressurized gas is supplied in this case.

- Simple cylindrical aerodynamic bearing
- Aerodynamic foil bearing
- Tilting pad aerodynamic bearing

The main disadvantage of the aerodynamic bearing is its low load carrying capacity as well as stiffness in comparison to the aerostatic bearing. Aerodynamic bearing is not suitable for the low speed operations as the unbalance, like whirl, is more. It is suitable only for continuous operations. If there is more stop and start cycles, then there may be more wear. The major thing is that its manufacturing procedure is very complex in comparison to the aerostatic bearing.

1.3.2 Aerostatic bearing:

In case of aerostatic bearing, external pressurized gas is supplied to the bearing clearance through feed holes of the bearing. Restrictor inside the feed hole helps the gas to expand. Then, in the clearance region, the gas again expands. There are mainly two types of aerostatic bearing, cylindrical journal bearing, thrust pad or thrust bearing. New type of

aerostatic bearing in tapered geometry was also invented which can work as combination of both cylindrical and thrust bearing. But, for that the shaft has to be tapered.

In case of case of horizontal shaft, the shaft will be at an eccentric position due to its own weight (Fig-1.1). So the clearance at the bottom will be more in comparison to the clearance at top. Hence the pressure difference between the inlet and outlet of feedhole will be less and so the flow rate. But, at top pressure difference will be more because of more clearance and so the flow rate. And this pressure difference between across the shaft pushes the shaft towards the high clearance region, which results floating of the shaft on the gas film layer. And this pressure differential produces the load capacity of the bearing. Multiplication of pressure and the projected area gives the force exerted due to the pressure.

The gas journal bearing can be operated in three different kinds of modes.

- Aerodynamic mode
- Purely aerostatic mode (supply of external pressurized gas with no rotation of shaft)
- Hybrid mode (supply of external pressurized gas with rotation of shaft)

Load carrying capacity of aerostatic bearings is more in comparison to the aerodynamic bearings, which results high stiffness. It is suitable for non-continuous operations as it gives good damping. Manufacturing process of this bearing is simple in compare to the aerodynamic bearing.

The pressure difference is created due to the flow restrictor placed inside the feedhole by reducing the supply pressure. The stiffness of the bearing is the result of this pressure difference. This can be achieved by using different types of restrictors. Some of the restrictors are given below.

- Inherent Compensation
- Pocketed orifice
- Slot entry
- Porous plug
- Porous linear
- Capillary
- Restricting land

Out of these restrictors, annular orifice, pocketed orifice and slot entry orifices are commonly used.

Among all these type of restrictors, orifice types of restrictors are easy to manufacture. Here pocketed orifice is considered as the load capacity is increased by 50 % in comparison to annular orifice [2].

1.4 Advantages of Aerostatic bearing:

- Zero Wear
- Negligible Friction
- Contamination free atmosphere
- High Speed Application
- Simple Design Process
- Applicable over a wide temperature range
- Less instability during rotation of the shaft

1.5 Disadvantages of Aerostatic bearing:

- Precision geometry and surface finish (from manufacturing point of view)
- Decrease in plant cycle efficiency

1.6 Aim of the present study:

The present study covers the analysis of the fluid flow through the feed holes, clearance of the hybrid journal bearing as well as that of thrust bearing. Dynamic unbalances like whirling, created due to the rotation of shaft are also covered in this work. The main aim of the present study is to make a simple procedure to study the different parameters for the control system for the bearing system.

2 LITERATURE REVIEW

2.1 History and Application

The gas bearing came into action around 18th century. The research on gas bearings further increased due to the wide application of the gas bearing like military hardware. The gas bearing is widely used in Gas Turbines, Naval Ships, aircrafts, Computer hard disks as well as small diameter Dental drillers, Cryogenic turbo-expanders. Gas bearings are also used in different manufacturing sectors vastly because of its precision in the field of high speed applications.

2.2 Different approaches made for the analysis of journal bearing

For the design of aerostatic journal bearings, different researchers suggested different methods. The present work is mainly based on the design procedure suggested by Powell [1] and Pink et al. [2]. According to Powell [1], maximum load capacity can be achieved by taking the value of the bearing pressure ratio, $((P_{do}-P_a)/ (P_o-P_a)) = K_{go} =0.4$. Whereas, M.T.I.[6] and Constantinescu[7] use a different method by introducing a parameter called 'feeding parameter' to describe the matching of flow resistances. Pink et al. [2] also referred the same feeding parameter. As the feeding parameter only depends on the geometrical parameters of the aerostatic journal bearing, this method is easy for the analysis of the optimum design conditions of the journal bearing, in comparison to the other method adopted by different researchers.

Here ε=0.5 has been taken as suggested by Powell [1] as at high eccentricity ratios, radial stiffness decreases.

The flow in the clearance is similar to that of flow between parallel plates.

The Navier-strokes equation for the flow through parallel flat plates is given by

$$\frac{\partial^2 u}{\partial y^2} = \frac{1}{\mu}\frac{\partial P}{\partial x} \tag{2.1}$$

Powell [1] made the following assumptions for the derivation of the expression for the fluid flow through the clearance

- The flow in the bearing clearance is assumed to be normal to the feeding plane.
- This implies one dimensional flow with pressure constant across the film and clearance, constant throughout the bearing.

- For double admission bearings, the pressure between the inlet planes is assumed constant.
- The flow through the bearing clearance is assumed to be purely viscous without slip at the boundaries. This means that the gas inertia is neglected.

The expression used for the total mass flow rate through bearing clearance is given by

$$\dot{M} = [(\frac{P_d}{P_0})^2 - (\frac{P_a}{P_0})^2]\frac{\pi h^3 {P_0}^2}{6 \mu R T \xi} \quad (2.2)$$

where, $\xi = \int_0^{y=Y} \frac{2\pi}{x}\, dy$

Variation of flow length dy with change in the flow width x is defined by the shape factor ξ.

By using the above equation, pressure drop can also be calculated. Multiplication of the pressure downstream of the throat and the projected area gives the force exerted by the pressurised gas on the shaft.

2.2.1 Radial load Capacity

And the vector sum of the vertical components of the radial forces gives the load carrying capacity of the bearing. But, Effects like dispersion effect, non-axial flow reduce the load capacity. There are different formulas to find out this coefficient.

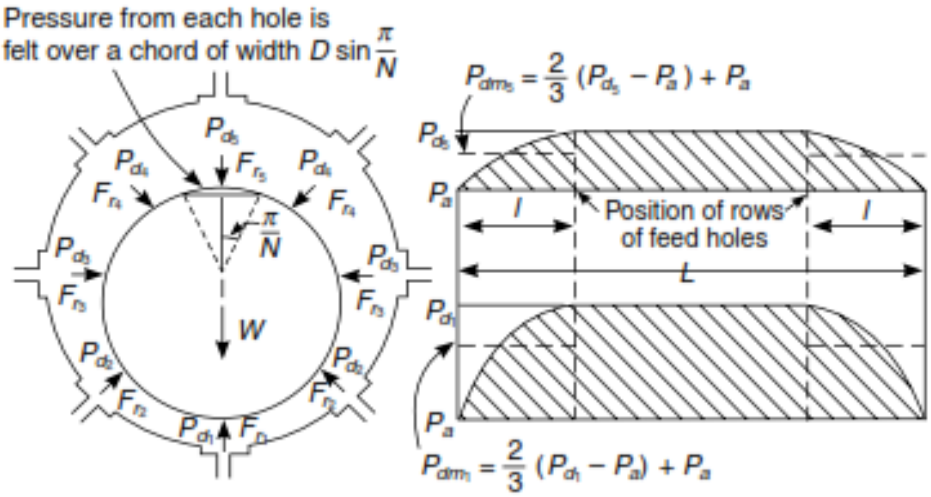

Figure 2.1: Pressure Distribution of Journal bearing [1]

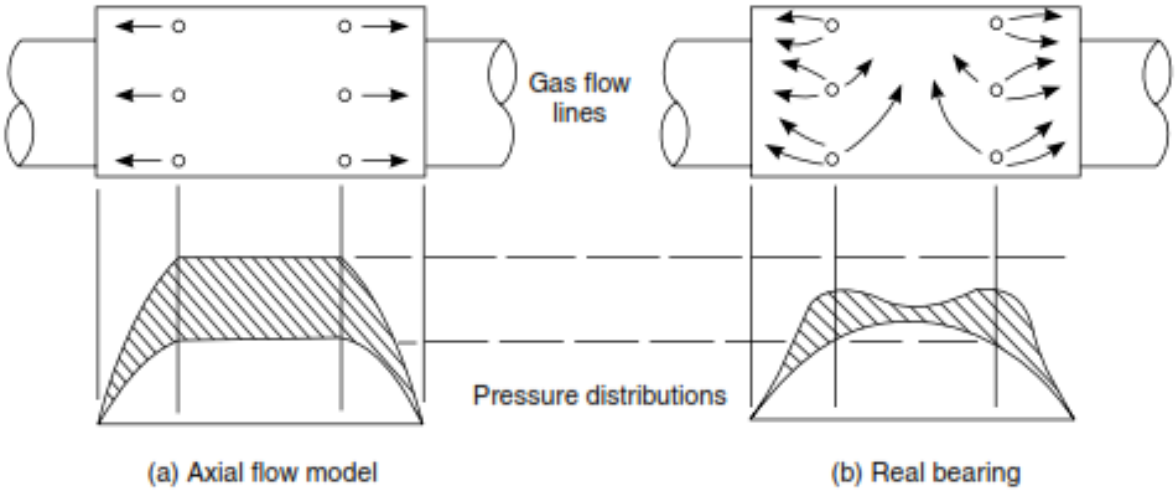

Figure 2.2: Flow of gas inside journal bearing clearance and pressure distribution [1]

Dudgeon and Lowe [5] have shown that the theoretical load is reduced by a factor C_w given by

$$C_w = 0.89 \frac{dn}{\prod D}^{0.21} \frac{Ln}{\prod D}^{0.42} \left(\frac{P_d}{p_0}\right)^{0.0505} \left(\frac{\prod D}{nd}\right)^{0.379} \left(\frac{\prod D}{nL}\right)^{0.758} \quad (2.3)$$

Shires [4] had given a formula to find out the non-axial flow coefficient C_L was derived from the experimental results of Robinson and Sperry [3], given by

$$\frac{C_L}{C_{L0}} = .315 \frac{\frac{\cosh\left(\frac{6.36l}{D}\right) - 1}{\sinh\left(\frac{6.36l}{D}\right)} + \tanh\left(6.36\frac{L-2l}{D}\right)}{\left(\frac{L-l}{D}\right)} \quad (2.4)$$

where,

$$C_{L0} = \frac{W}{(P_0 - P_a)LD}$$

The aerostatic Radial Stiffness can be calculated by using the formula (K) = $\frac{\partial W}{\partial \mathrm{h}}$

2.2.2 Aerodynamic Performance of hybrid journal bearing

In the hybrid mode of operation, it was found that the aerodynamic effect due to the rotation of the journal can increase the load capacity of the bearing. An approximation aerodynamic load capacity calculation was done by Powell [1].

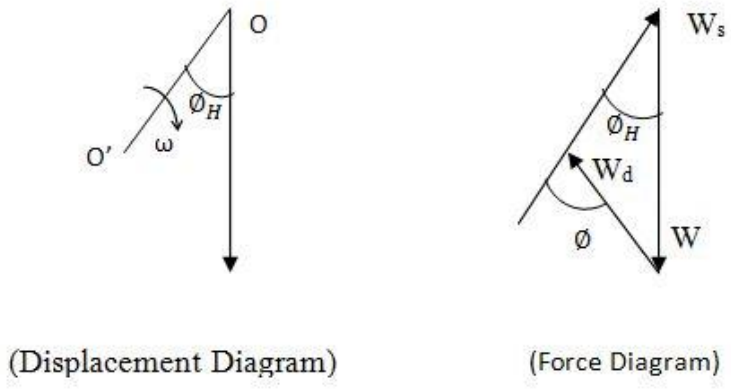

Figure 2.3: Force and Displacement Diagram of shaft [1]

The resultant load capacity of the hybrid journal bearing can be found out by using the above force diagram and so the overall stiffness.

Powell [1] introduced a constant as Compressibility Number

$$\Lambda_H = \frac{\mu\omega}{P_m}\left(\frac{a}{h_0}\right)^2 \tag{2.5}$$

where,

P_m is the mean pressure defined as $P_m = \frac{P_O + P_a}{2}$ (2.6)

From the force diagram, Powell [1] derived a formula to find out the overall load capacity.

$$W = W_s \cos \emptyset_H + W_d \cos(\emptyset - \emptyset_H) \tag{2.7}$$

and

$$\cot \emptyset_H = \frac{W_s}{W_d \sin \emptyset} + \cot \emptyset \tag{2.8}$$

2.3 Thrust Bearing

Here, the flow through the clearance of the thrust bearing is similar to that of flow between two circular plates, where the inward flow is towards the centre of the bearing and then coming out radially.

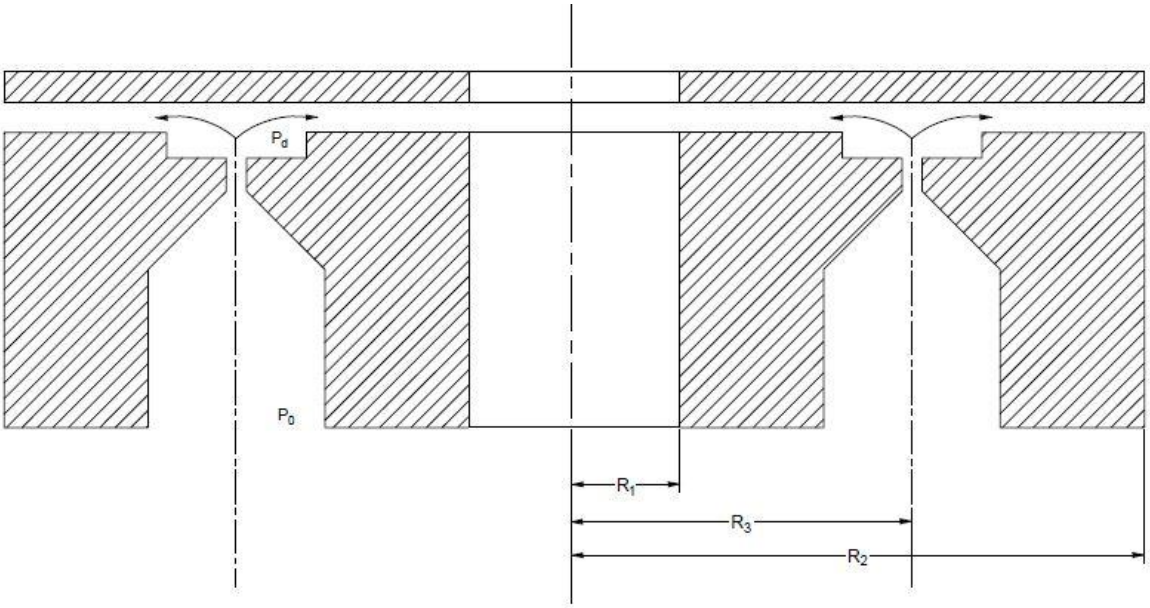

Figure 2.4: Sectional View of Annular thrust Bearing and shaft collar

The expression can be found out from the equation

$$\frac{\partial^2 u}{\partial y^2} = \frac{1}{\mu}\frac{\partial P}{\partial r} \tag{2.9}$$

In case of thrust pad, the following expression can be used for the pressure drop as well as mass flow rate, derived from the equation.

$$P_d{}^2 - P_a{}^2 = \frac{12\,\mu\, m\, R\, T}{\Pi\, h^3}\log\frac{R_2}{R_1} \tag{2.10}$$

But for the annular thrust bearing, there will be two different paths for the fluid come out, towards the journal (inward flow) and away from the journal (outward flow).

For the inward flow,

$$m_2 = \frac{\left(P_d{}^2 - P_a{}^2\right)\Pi\, h^3}{12\,\mu\, R\, T\log\left(\frac{R_3}{R_1}\right)} \tag{2.11}$$

For the outward flow,

$$m_1 = \frac{\left(P_d{}^2 - P_a{}^2\right)\Pi\, h^3}{12\,\mu\, R\, T\log\left(\frac{R_2}{R_3}\right)} \tag{2.12}$$

Here, for the same values of m_1 and m_2, $\frac{R_2}{R_3} = \frac{R_3}{R_1}$

So the total mass flow rate,

$$M = \frac{(P_d{}^2 - P_a{}^2)\, \Pi\, h^3}{6\, \mu\, R\, T \log\left(\frac{R_2}{R_1}\right)} \tag{2.13}$$

For the load capacity calculation, Powell [1] derived one formula by introducing a factor K_g.

where,

$$K_g = \frac{2}{1 + \left(1 + \frac{4}{G^2}\right)^{1/2}} \tag{2.14}$$

and 'G', called as slot factor

$$= \frac{P_a/P_0}{(1 - P_a/P_0)^{1/2}\,(1 + P_a/P_0)} \times \frac{24\, \mu\, (2\, R\, T)^{1/2}}{P_a} \times \frac{C_D\, n d^2 \log\left(R_2/R_1\right)}{8\, h^3} \tag{2.15}$$

For the load capacity, the following expression can be used

$$W = \frac{K_g\, (P_0 - P_a)\, \Pi\, (R_2 - R_1)^2}{\log(R_2/R_1)} \tag{2.16}$$

2.4 Different modern bearings

To support the rotation of shaft, generally two cylindrical journal bearings and two thrust bearings are used in combine. But, an alternative method was studied by Pande, S. S. et al. [1982], by using tapered bearing. This tapered bearing acts as the combination of cylindrical journal bearing and thrust bearing. But for this, the geometry of the shaft has to be tapered.

But, recently there is another effective bearing is being used, magnetic bearing, suitable for high speed and very high speed applications.

3 DESIGN PROCEDURE

3.1 Elements of Turbo-expander:

The turbo-expander essentially consists of a Turbo-expander wheel and a brake compressor mounted on a single shaft, supported by the required number of journal and thrust bearings. These basic components are held in place by an appropriate housing, which also contains the fluid inlet and exit ducts.

1. Turbo-expander wheel
2. Brake compressor
3. Shaft
4. Nozzle
5. Journal Bearings
6. Thrust bearings
7. Diffuser
8. Bearing Housing
9. Cold end housing
10. Warm end housing
11. Seals

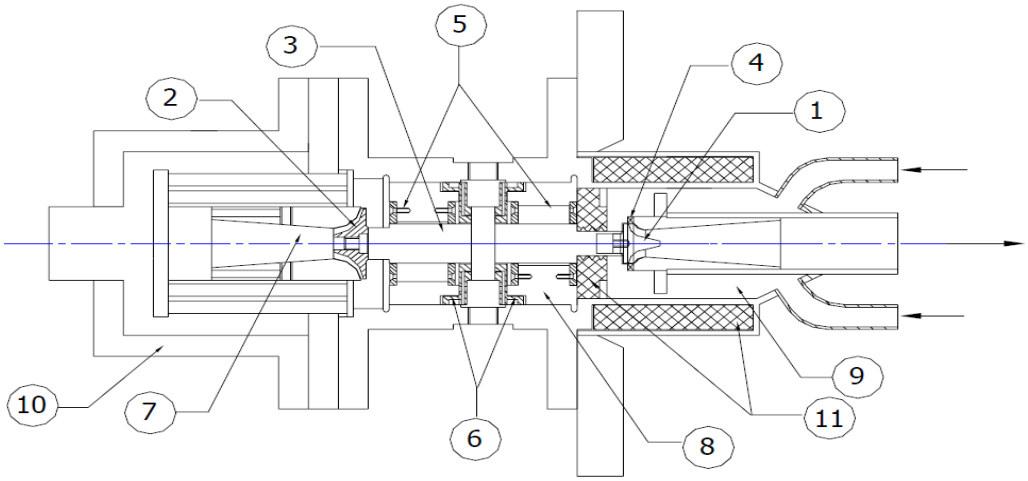

Figure 3.1: Schematic diagram of Turbo-expander [12]

As in this case, the rotor is horizontal, so the journal bearings are supposed to do the additional task of supporting the horizontal rotor weight. The shaft collar, along with the thrust plates, form a pair of thrust bearings that take up the load due to the difference of pressure between the Turbo-expander and the compressor ends. The supporting structures

mainly consist of the cold and the warm end housings with an intermediate thermal isolation section. They support the static parts of the turbo-expander assembly, such as the bearings, the inlet and exit ducts and the speed and vibration probes. But in a vertical rotor, the thrust bearings used to support the rotor weight.

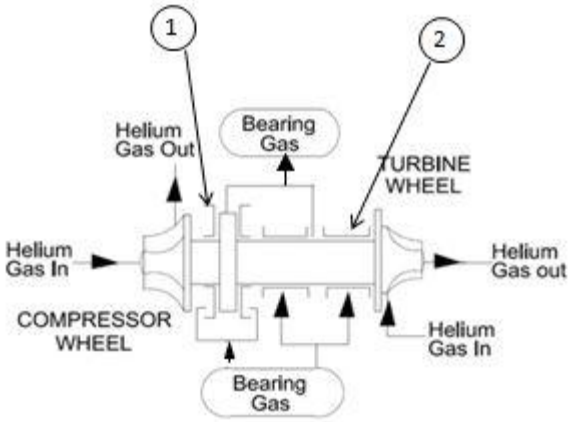

Figure 3.2: Gas flow path of Turbo-expander and Bearing system

3.2 Design Considerations

Powell [1] found that the optimum conditions for the journal bearing were at L/D ratio=1, n=8. And ε=0.5 has been taken as at high eccentricity ratios, radial stiffness decreases.

In order to avoid pneumatic hammer, and to limit dispersion effect, Pink [2] suggested some design criteria.

- To avoid pneumatic hammer

$$\frac{Nbd_R{}^2}{4DLh_0} \leq .05$$

- For limiting dispersion effect

$$d_R \geq \frac{7.77D}{n^3\left(\frac{L}{D}\right)^2}$$

According to Powell [1], the maximum mass flow rate at restrictors as it may leads to pneumatic hammer. So, here the design is done by restricting the maximum mass flow rate at every feedhole.

Here some typical parameters of shaft and bearing have been considered for the design.

L=15 mm, D=15 mm, L_s=110 mm, m_R=0.16Kg

3.3 Design Procedure of Feed hole

According to the systems available at IPR, the maximum inlet pressure and the outlet pressure have been considered as 12 bar and 1.2 bar respectively. The present work confined to different values of radial clearance in the range 9-20 µm, values of orifice diameter in the range of 0.07-0.2 mm and for different values of inlet and outlet pressure.

The flow through the feed hole is assumed as isentropic process, i.e. the expansion of gas from supply pressure to the throat pressure is reversible adiabatic process. Two pressure losses occur downstream of the throat of the orifice flow area, the first occurs at the orifice curtain area $\pi d_0(b + h)$ and the second at the entrance to the bearing film flow area $\pi d_R h$.

The throat pressure can be calculated by equating the total flow through all the feed holes to the flow through the bearing clearance.

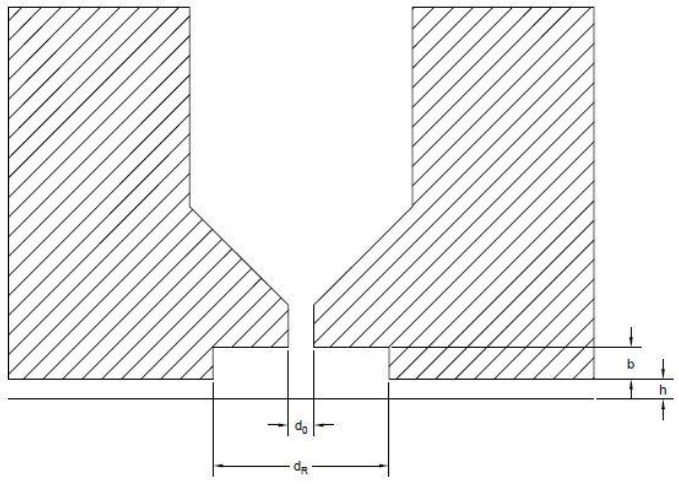

Figure 3.3: Sectional view of feedhole

The mass flow rate through one feed hole can be expressed by

$$\dot{m}_0 = C_d \frac{\pi {d_0}^2}{4\sqrt{1+{\delta_L}^2}} P_0 \left[\frac{2\Upsilon}{(\Upsilon-1)RT}\left\{\left(\frac{P_t}{P_0}\right)^{\frac{2}{\Upsilon}} - \left(\frac{P_t}{P_0}\right)^{\frac{\Upsilon+1}{\Upsilon}}\right\}\right]^{1/2} \quad (3.1)$$

where,

$$\delta_L = \frac{1}{4}\left[\left(\frac{{d_0}^2}{d_R\, h}\right)^2 + \left(\frac{d_0}{b+h}\right)^2\right]^{1/2}, \tag{3.2}$$

It is the ratio of the orifice flow area $\frac{\pi\, {d_0}^2}{4}$ to the curtain flow area $\pi d_o h$.

$$\frac{P_t}{P_0} = \left(\frac{2}{\Upsilon+1}\right)^{\Upsilon/\Upsilon-1}, \text{ for choked flow}$$

$$= \frac{P_d}{P_0}, \text{ for subsonic flow}$$

The parameter δ_L, is the ratio of the orifice flow area $\frac{\pi\, {d_0}^2}{4}$ to the curtain flow area $\pi d_o h$.

As suggested by Powell [1], the value of C_d is generally taken as 0.8.

3.4 Design Procedure of Hybrid journal Bearing

3.4.1 Mass flow rate Calculation

The mass flow rate through one feedhole is given by the equation 3.3.

$$\dot{m}_0 = C_d \frac{\pi\, {d_0}^2}{4\sqrt{1+{\delta_L}^2}} P_0\left[\frac{2\,\Upsilon}{(\Upsilon-1)RT}\left\{\left(\frac{P_t}{P_0}\right)^{\frac{2}{\Upsilon}} - \left(\frac{P_t}{P_0}\right)^{\frac{\Upsilon+1}{\Upsilon}}\right\}\right]^{1/2} \tag{3.3}$$

and the mass flow rate through bearing clearance is given in the equation 3.4.

$$\dot{M} = \left[\left(\frac{P_d}{P_0}\right)^2 - \left(\frac{P_a}{P_0}\right)^2\right]\frac{\pi\, h^3 {P_0}^2}{6\,\mu\, R\, T\, \xi} \tag{3.4}$$

By equating equation 3.3 and 3.4,

$$C_d \frac{\pi\, {d_0}^2}{4\sqrt{1+{\delta_L}^2}} .N. P_0 \left[\frac{2\,\Upsilon}{(\Upsilon-1)RT}\left\{\left(\frac{P_t}{P_0}\right)^{\frac{2}{\Upsilon}} - \left(\frac{P_t}{P_0}\right)^{\frac{\Upsilon+1}{\Upsilon}}\right\}\right]^{1/2}$$

$$= \left[\left(\frac{P_d}{P_0}\right)^2 - \left(\frac{P_a}{P_0}\right)^2\right]\frac{\pi\, h^3 {P_0}^2}{6\,\mu\, R\, T\, \xi}$$

or, $$\Lambda_s \xi \left[\frac{2\,\Upsilon}{(\Upsilon-1)}\left\{\left(\frac{P_t}{P_0}\right)^{\frac{2}{\Upsilon}} - \left(\frac{P_t}{P_0}\right)^{\frac{\Upsilon+1}{\Upsilon}}\right\}\right]^{1/2}$$

$$= \left[\left(\frac{P_d}{P_0}\right)^2 - \left(\frac{P_a}{P_0}\right)^2\right] \tag{3.5}$$

where,

$\Lambda_s\xi$ is called the feeding parameter

$$= \frac{C_d\ 6\ \mu\ \sqrt{RT}\ N\ {d_0}^2}{4\sqrt{1+{\delta_L}^2}\ .P_0\ \ h^3}\ \xi$$

As the feeding parameter only depends on the geometrical parameters, its value can be calculated from the geometry of the feeding system of the bearing.

3.4.2 Static load Capacity Calculation

By using the equation 3.5, pressure drop can also be calculated. Multiplication of the pressure downstream of the throat and the projected area gives the force exerted by the pressurised gas on the shaft.

And the vector sum of the vertical components of the radial forces gives the load carrying capacity of the bearing.

Radial force,

$$F_r = P_d(L-2l)Dsin\frac{\pi}{N} + 2\left[\left[\frac{2}{3}(P_d - P_a) + P_a\right] lDsin\frac{\pi}{N}\right] \quad (3.6)$$

Load Capacity,

$$W = F_{r1} - F_{r5} + 2(F_{r2} - F_{r4})\ cos\frac{\pi}{4} \quad (3.7)$$

3.4.3 Radial Stiffness Calculation of Hybrid Journal Bearing

Radial Stiffness (K) = $\frac{\partial W}{\partial h}$ (3.8)

3.4.4 Aerodynamic load Calculation

In the hybrid mode of operation, it was found that the aerodynamic effect due to the rotation of the journal can increase the load capacity of the bearing. An approximation aerodynamic load capacity calculation was done by Powell [1].

3.4.5 Overall load capacity and Stiffness Calculation

The resultant load capacity of the hybrid journal bearing can be found out by using the above force diagram and so the overall stiffness.

3.5 Design Procedure of Thrust Bearing

3.5.1 Mass Flow rate Calculation

The mass flow rate can be calculated by using the formula mentioned in chapter 2.4.

$$M = \frac{\left(P_d{}^2 - P_a{}^2\right) \Pi\, h^3}{6\,\mu\, R\, T \log\left(\frac{R_2}{R_1}\right)} \tag{3.9}$$

3.5.2 Load Capacity and Stiffness Calculation

For load capacity calculation, equations 2.16, 2.15, 2.14 can be used.

$$W = \frac{K_g\,(P_0 - P_a)\,\Pi\,(R_2 - R_1)^2}{\log(R_2/R_1)} \tag{3.10}$$

where, $K_g = \frac{2}{1+\left(1+\frac{4}{G^2}\right)^{1/2}}$ (3.11)

and $G = \frac{P_a/P_0}{(1-P_a/P_0)^{1/2}\,(1+P_a/P_0)} \frac{24\,\mu\,(2\,R\,T)^{1/2}}{P_a} \frac{C_D\,n d^2 \log\left({}^{R_2}/_{R_1}\right)}{8\,h^3}$ (3.12)

3.6 Dynamic Analysis of the Shaft

The main part of the bearing is the dynamic analysis of the shaft to check the displacement of shaft during rotation. As the displacement or whirling of shaft depends mainly upon the stiffness of the bearing, the dynamic analysis is like crosschecking of the initial design done previously. Here the design is done according to Powell [1].

The following assumptions were made by Powell [1] for the easy mathematics.

- The shaft is purely rigid and the bearings used here are rigidly supported. So, only finite amount of stiffness and damping will be there.
- From aerodynamic point of view, the bearings operate in the incompressible regions.
- Squeeze film action and aerodynamic effect are the only reasons of damping.

The dimensionless damping force can be represented as

$$\bar{W} = \frac{W}{L\,D\,P_a} = \bar{W}_{sf} - \bar{W}_d \tag{3.13}$$

where

$$\bar{W}_{sf} = \frac{6\,\Pi}{(1-\varepsilon^{2})^{3/2}} \frac{\Pi}{h_0} \left(\frac{\Lambda}{w}\right) \omega^{*} \tag{3.14}$$

$$\bar{W}_{d} = \frac{6\,\Pi}{(2+\varepsilon^{2})(1-\varepsilon^{2})^{1/2}} \frac{\Pi}{h_0} \left(\frac{\Lambda}{w}\right) \omega \tag{3.15}$$

$$\Lambda = \frac{\mu\,\omega}{P_a} \left(\frac{a}{h_0}\right)^{2} \tag{3.16}$$

and then, the damping coefficient 'C' can be found out by $C = \frac{W}{r\omega}$

Here, two journal bearings are used to support the rotation of the turbo-expander as well as its weight. So for the smooth rotation of the shaft, the damping forces, stiffness of the two hybrid journal bearings are responsible to control the unbalances created during rotation.

The motion of the shaft is represented by the following equations.

$$m_R \frac{d^2x}{dt^2} + 2m_R\eta \frac{dx}{dt} + 2Kx = X\omega^2 \sin\omega t \tag{3.17}$$

$$(I - I_0)\frac{d^2\beta}{dt^2} + 2m_R\eta J^2 \frac{d\beta}{dt} + 2KJ^2\beta = Y\omega^2 \sin\omega t \tag{3.18}$$

where,

$$x = \frac{X\omega^2 \sin(\omega t - \delta_1)}{m_R\,[(\omega_1{}^2 - \omega^2)^2 + 4\omega^2\eta^2\,]^{1/2}}$$

$$\delta_1 = tan^{-1}\left[\frac{2\omega\eta}{m_R\,(\omega_1{}^2 - \omega^2)}\right]$$

$$\omega_1{}^2 = \frac{2K}{m_R}$$

$$\beta = \frac{Y\omega^2 \sin(\omega t - \delta_2)}{(I - I_0)\left[(\omega_2{}^2 - \omega^2)^2 + \frac{4\,m_R{}^2\eta^2 J^4\omega^2}{(I - I_0)^2}\right]^{1/2}}$$

$$\delta_2 = tan^{-1}\left[\frac{2\,m_R\,\eta J^2\,\omega}{(I - I_0)(\omega_2{}^2 - \omega^2)}\right]$$

$$\omega_2{}^2 = \frac{2KJ^2}{(I - I_0)}$$

In the absence of damping, at resonant speed, the equation for the radial forces will be

$$2Kr = X\omega^2 + m_R\, r\omega^2 \tag{3.19}$$

$$r = \frac{X\omega^2}{(2\,K - m_R\omega^2)} \tag{3.20}$$

So the value of 'r' will reach maximum, when $2\,K - m_R\omega^2 = 0$

This occurs when $\omega_1{}^2 = \frac{2K}{m_R}$

But in real, damping is there. So the unbalance will be balanced by the damping force at the cylindrical resonance.

$$X\omega_1{}^2 = 2Cr\omega_1$$

$$r = \frac{X\omega_1}{2C} \tag{3.21}$$

This is the permissible limit of the whirling of shaft. Similarly, permissible limit of tilt angle can be set as given by the equation below.

$$\frac{r}{J} = \beta = \frac{Y\omega_2}{2C\,J^2} \tag{3.22}$$

Powell [1] stated that when the damping becomes zero, a self-excited whirl arises. The damping becomes zero when

$$\frac{\omega}{\omega^*} = \frac{2+\varepsilon^2}{1-\varepsilon^2} \tag{3.23}$$

The rotor will vibrate at two of its natural frequencies ω_1 and ω_2, due to any sudden load or disturbance. In case of the absence of forced vibration, ω^* will take the values of ω_1 or ω_2. But, generally it takes the lower natural frequency value.

Assuming the lower natural frequency to be in the cylindrical mode, the onset speed of the self excited whirl can be expressed as

$$\omega_c = \omega_1 \frac{2+\varepsilon^2}{1-\varepsilon^2} \tag{3.24}$$

In this case, ε=0.5 has been taken. So the above equation will become

$$\omega_c = 3\omega_1 \tag{3.25}$$

4 RESULT AND ANALYSIS

4.1 Journal Bearing

For the analysis of hybrid journal bearing, different geometrical parameters as well as different supply pressures and outlet pressures have been considered. Different graphs have been shown based on the results found from the analysis.

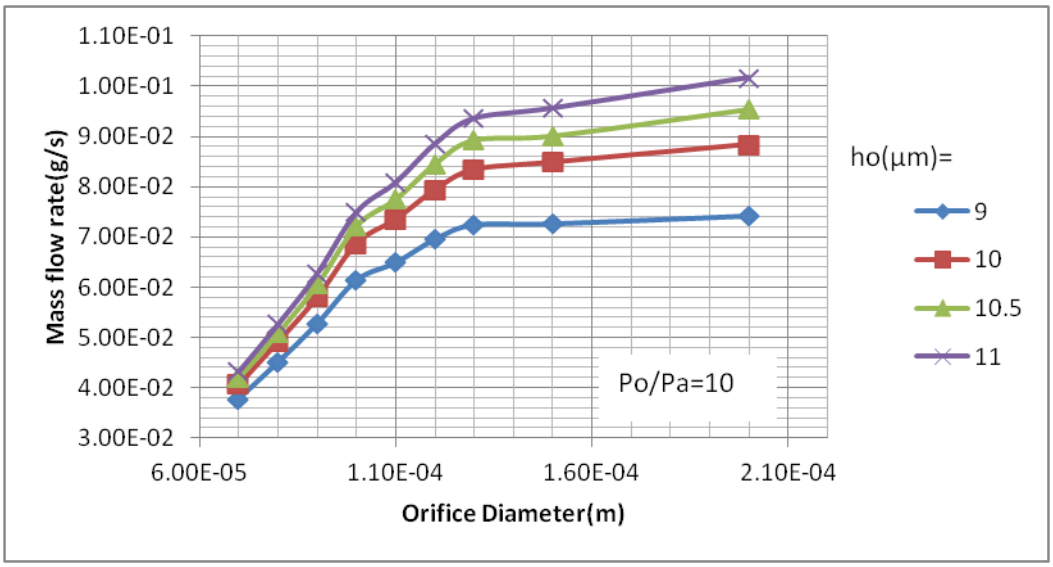

Figure 4.1: Effect of orifice Radius and radial clearance on Mass flow rate

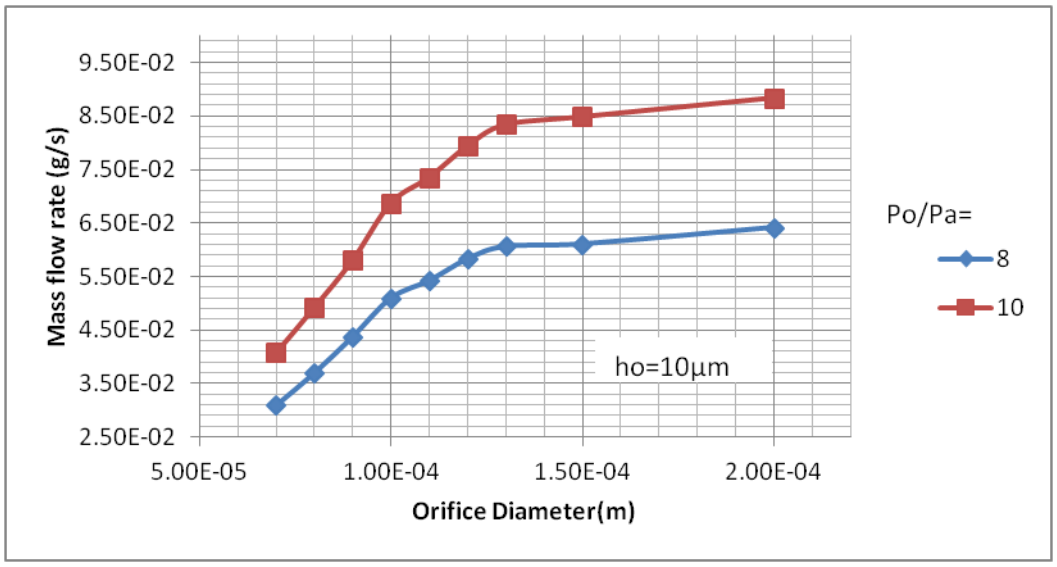

Figure 4.2: Effect of Pressure ratio P_o/P_a on Mass flow rate

It was found that the mass flow rate increases with increase in the diameter of the orifice. Initially, the mass flow rate increases rapidly with increase in orifice diameter, as shown in the Figure 4.1. But, after some value it increases slowly. And with increase in clearance, the mass flow rate also increases. But, after some value it increases slowly as choked flow

condition arises. The ratio of supply pressure to outlet pressure is another factor. With increase in pressure ratio, the mass flow rate also increases shown in figure 4.2.

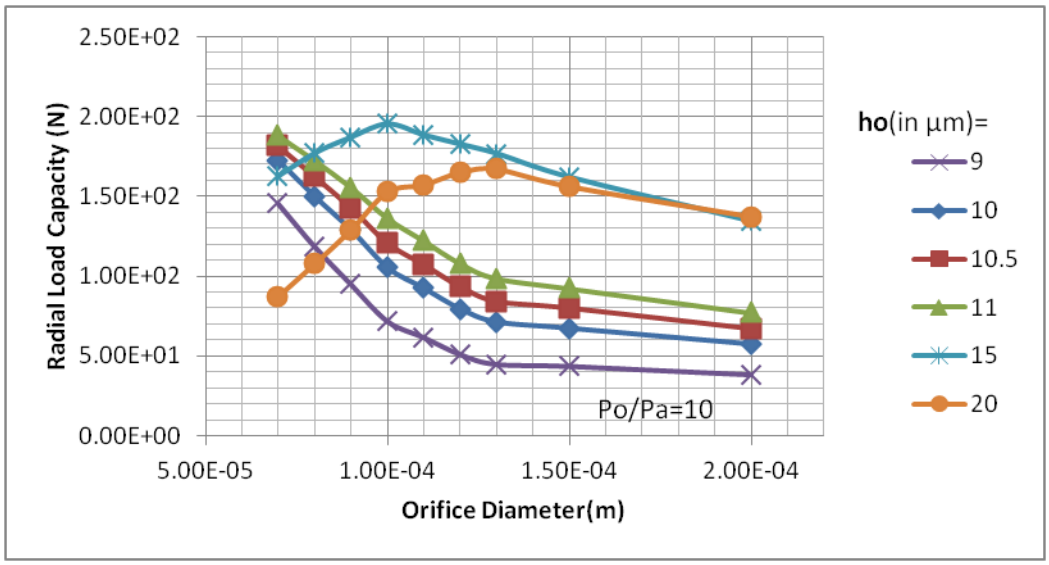

Figure 4.3: Effect of radial clearance on Radial Load Capacity

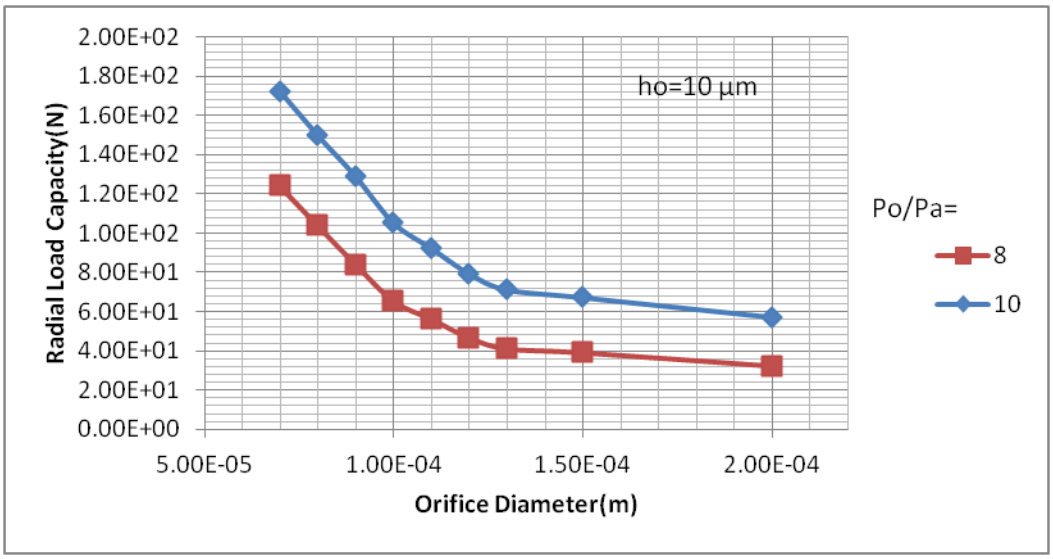

Figure 4.4: Effect of pressure ratio on Radial Load Capacity

From the Figure 4.3, it can be observed that the radial load capacity of the journal bearing increases with increase in radial clearance. But after some value it starts to decrease. Here, the radial load capacity increased from the clearance of 9µm to 11µm. At clearance 15µm, the load carrying capacity decreased after increasing for different values of orifice diameter

in the range of 7.00E-05m to 2.00E-04m. With increase in the supply pressure P_o, the load capacity also increases as shown in Figure 4.4 (P_a = 1.2 bar).

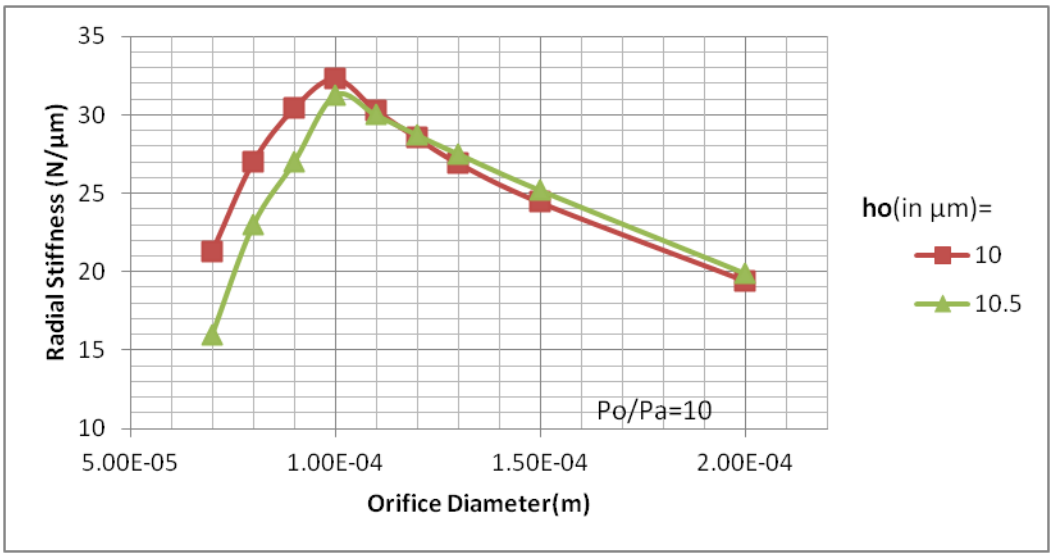

Figure 4.5: Effect of radial clearance on Radial Stiffness

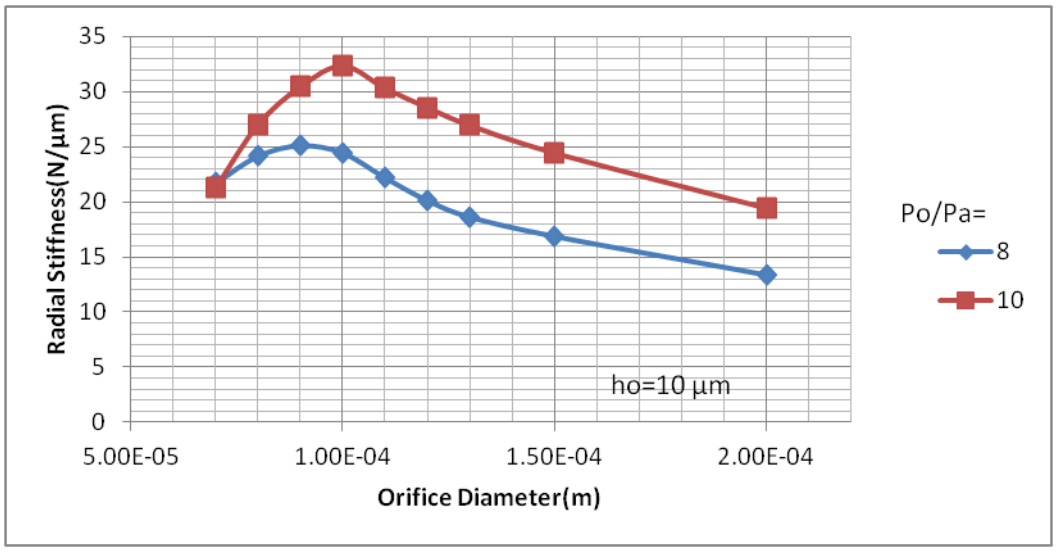

Figure 4.6: Effect of pressure ratio on Radial Stiffness

Though the mass flow rate increases with the increase in orifice diameter, but the load carrying capacity decreases as shown in Figure 4.2. The Figure 4.3 shows that by restricting the orifice diameter to a lower optimum value, we can achieve higher stiffness.

With high supply pressure, we can also get higher stiffness as shown in Figure 4.6. In case of journal bearing, the stiffness value increases and then decreases sown in Figure 4.5 and 4.6.

The radial stiffness of the journal bearing decreases with increase in radial clearance as shown in Figure 4.5.

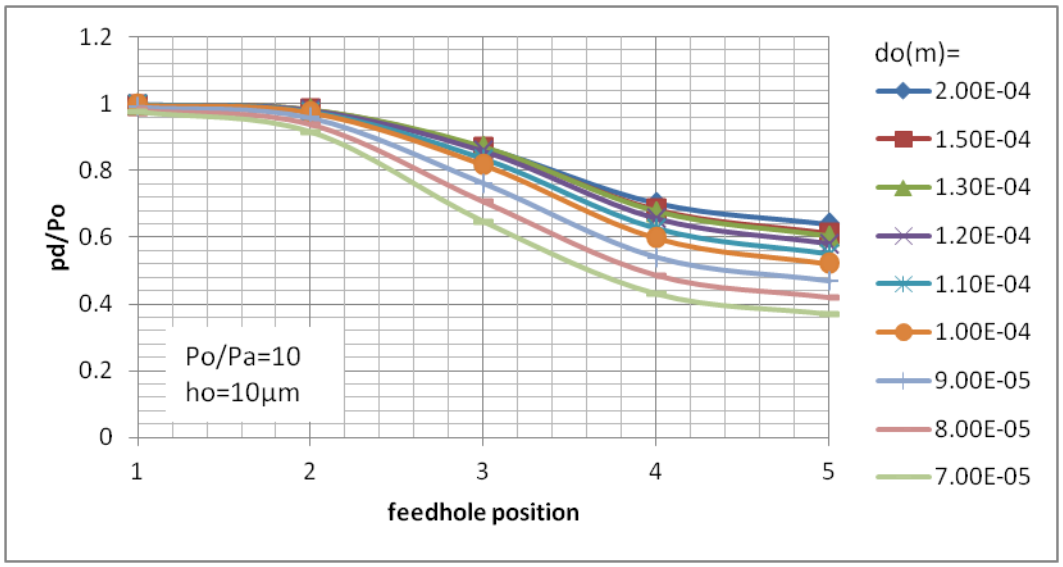

Figure 4.7: Values of P_d/Po at different feedhole positions

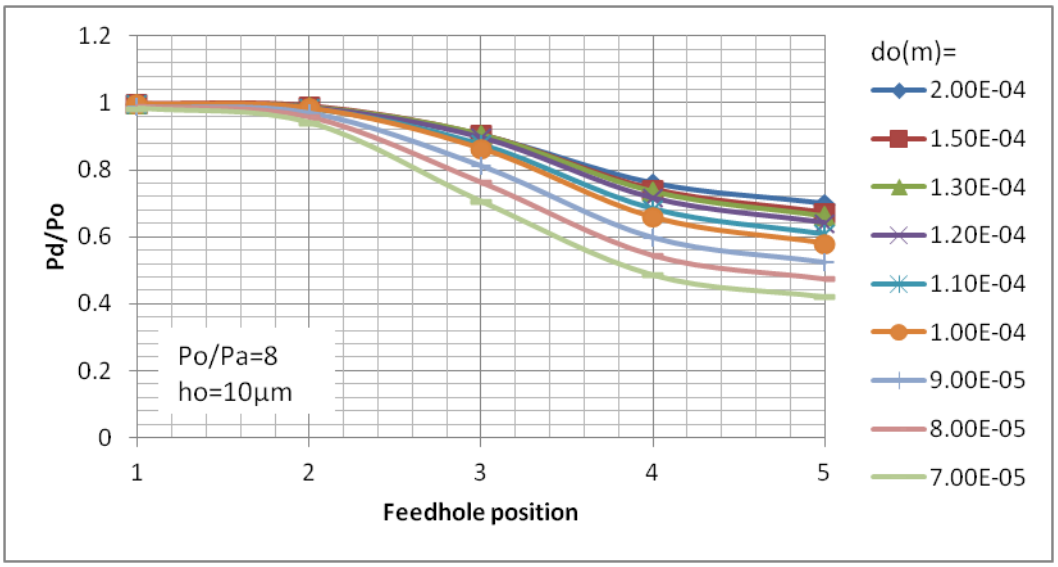

Figure 4.8: Values of P_d/P_o at different feedhole positions

Figures 4.7 and 4.8 show the graphs between different values of P_d/P_o at different feedhole positions shown in figure 2.1. It can be observed that at the low clearance side the expansion of gas occurs less because of flow restriction, whereas at the high clearance side, the expansion is more as there is more space for gas to expand. In order to restrict the maximum mass flow rate condition, the value of P_d/P_o should have to be greater than $(\frac{2}{\gamma+1})^{\gamma/\gamma-1}$, as described in chapter 3.3. As here, this work is done for helium gas, so the value of P_d/P_o should have to be greater than 0.4867. The value of γ has been taken from NIST chemistry web book [13].

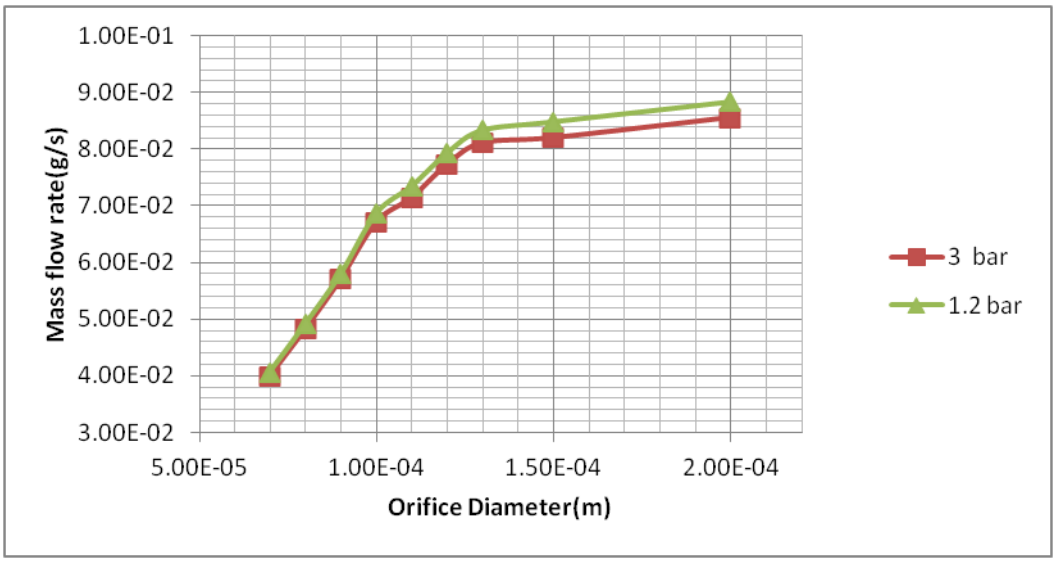

Figure 4.9: Effect of outlet pressure on Mass flow rate

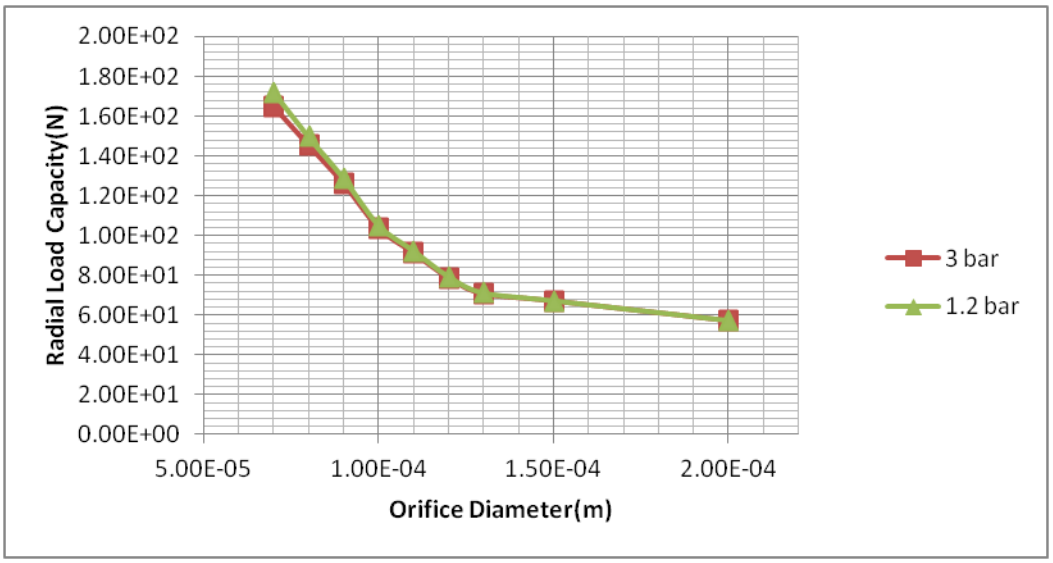

Figure 4.10: Effect of outlet pressure on Radial Load Capacity

Figures 4.9 and 4.10 show the variation of mass flow rate and Radial load capacity for different values of outlet pressure, respectively. Here the inlet pressure was kept constant as 12bar. And the outlet pressure was varied for specific geometrical parameters. The mass flow rate decreased with increase in outlet pressure and same the load capacity. But, increasing the outlet pressure also results choked flow at some feedholes. So, in order to avoid pneumatic hammer, we have to avoid those situations.

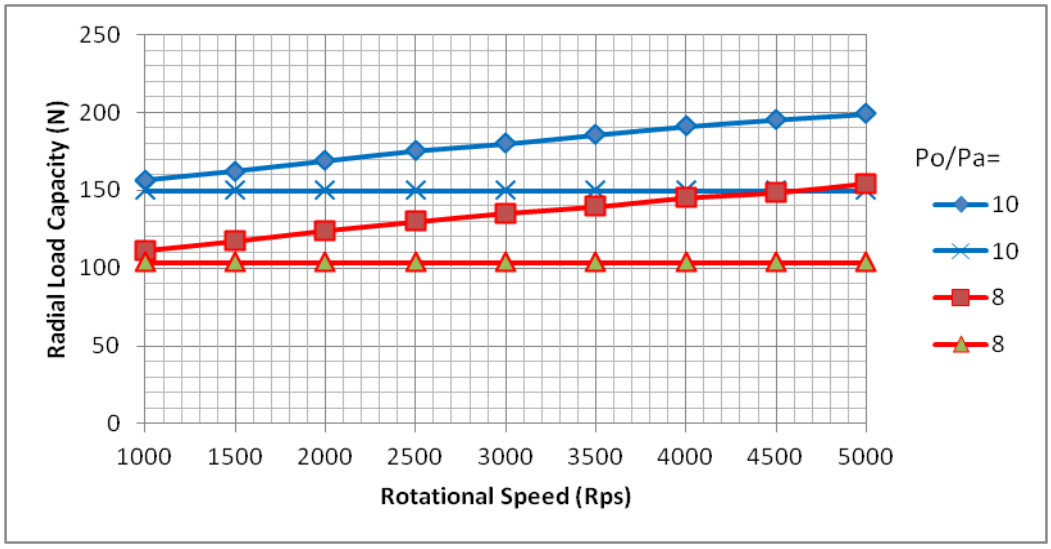

Figure 4.11: Effect of rotational speed on Overall Radial Load capacity

Because of the aerodynamic effect, the radial load carrying capacity of the hybrid journal bearing increases. Figure 4.11 shows the graph between overall load capacity and rotational speed, as well as the static load capacity for different values of pressure ratio P_o/P_a.

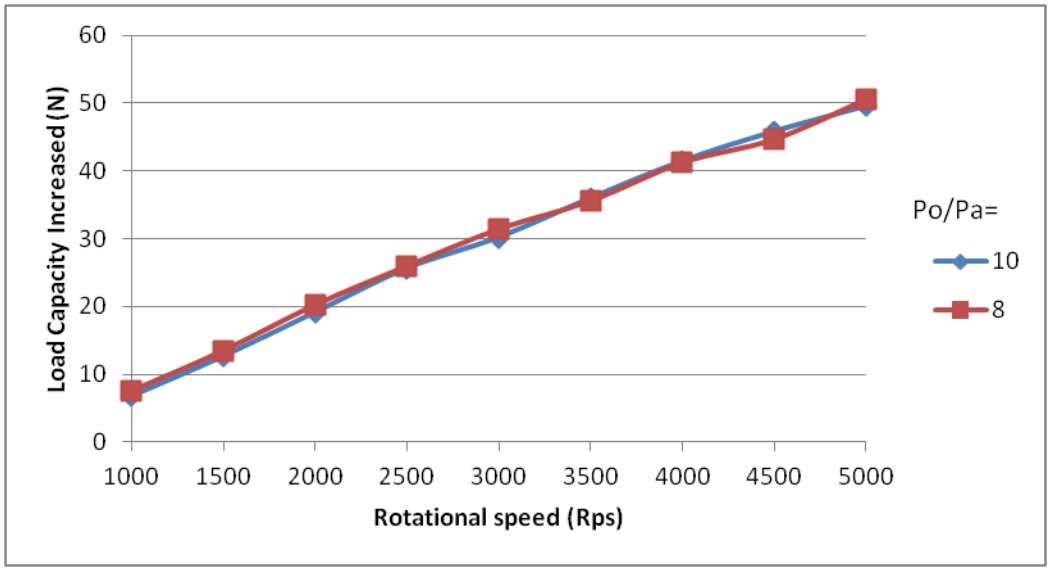

Figure 4.12: Effect of Rotational speed on Radial Load capacity Increased

From the figure 4.12, it can be observed that the aerodynamic load increases with increase in rotational speed. By decreasing the clearance, aerodynamic load can be increased. It can be concluded that bearings with higher diameter and less clearance results more aerodynamic load at higher rotational speed. The Figure 4.9 shows that the load increased due to aerodynamic effect at different P_o/P_a values nearly equal. As in this case, the values of P/P_m and ϕ have been taken from the graphs of Raimondi [11], so there is some deviations are coming. So, from this figure 4.9, it was found that the load increased due to the aerodynamic effect of journal bearing is independent of supply pressure.

4.2 Thrust Bearing

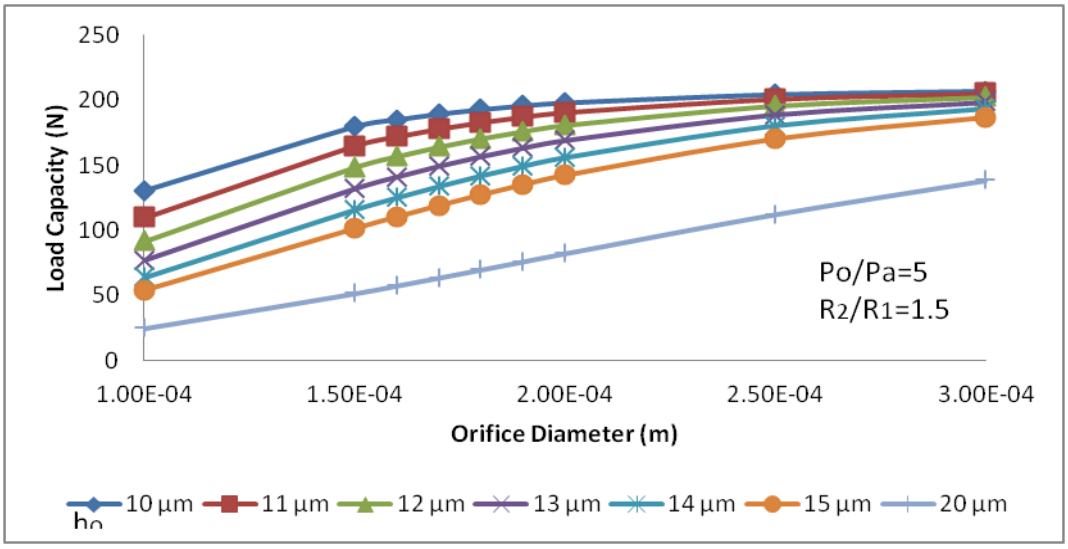

Figure 4.13: Effect of Orifice diameter and clearance on Load Capacity

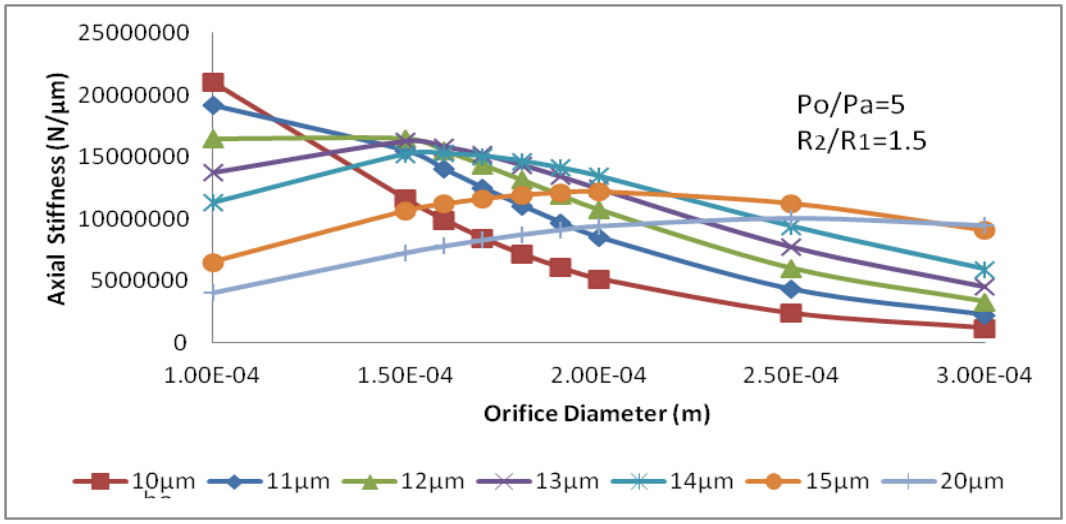

Figure 4.14: Effect of Orifice diameter and clearance on Axial Stiffness

In case of thrust bearing, the axial load capacity increases with increase in orifice diameter, whereas it decreases with increases in clearance as shown in Figure 4.13.

Figure 4.14 shows that the axial stiffness of the thrust bearing increases with increase in orifice diameter. And after some value it starts to decrease.

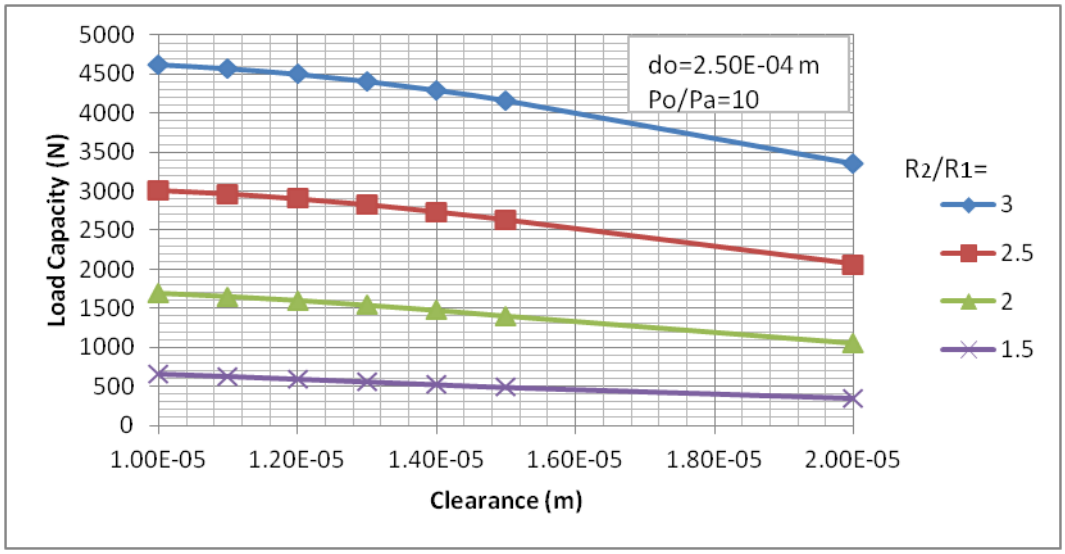

Figure 4.15: Load Capacity Vs Clearance for different R_2/R_1 values

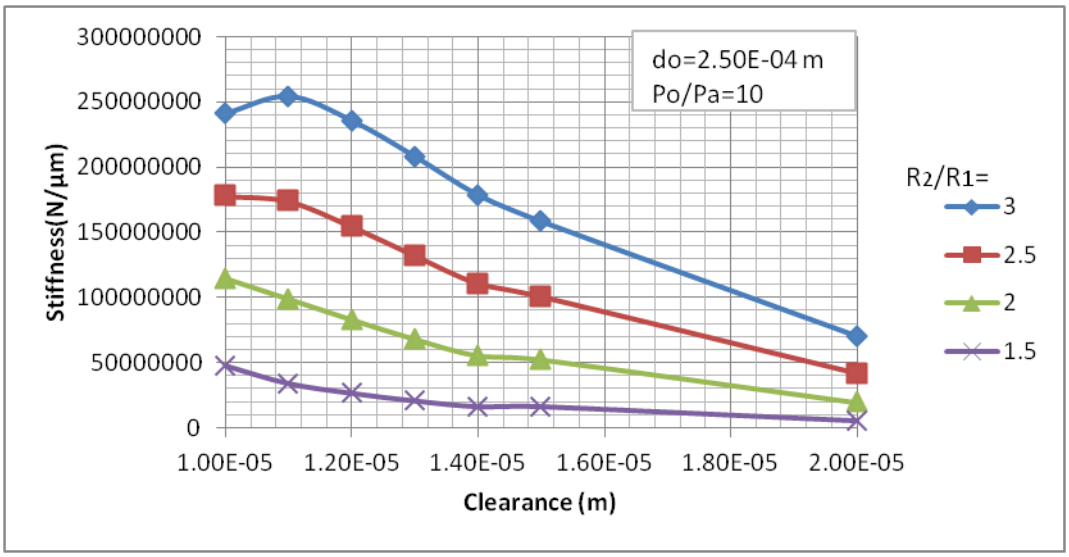

Figure 4.16: Stiffness Vs Clearance for different R_2/R_1 values

Figure 4.15 shows the variation of axial load capacity with different R_2/R_1 values. Axial load capacity of the thrust bearing increases with increases with increase in R_2/R_1 value. With

increase in clearance, the load capacity of the thrust bearing decreases as shown in the Figure 4.15. Axial stiffness varies in the same way as axial load capacity with R_2/R_1 and clearance.

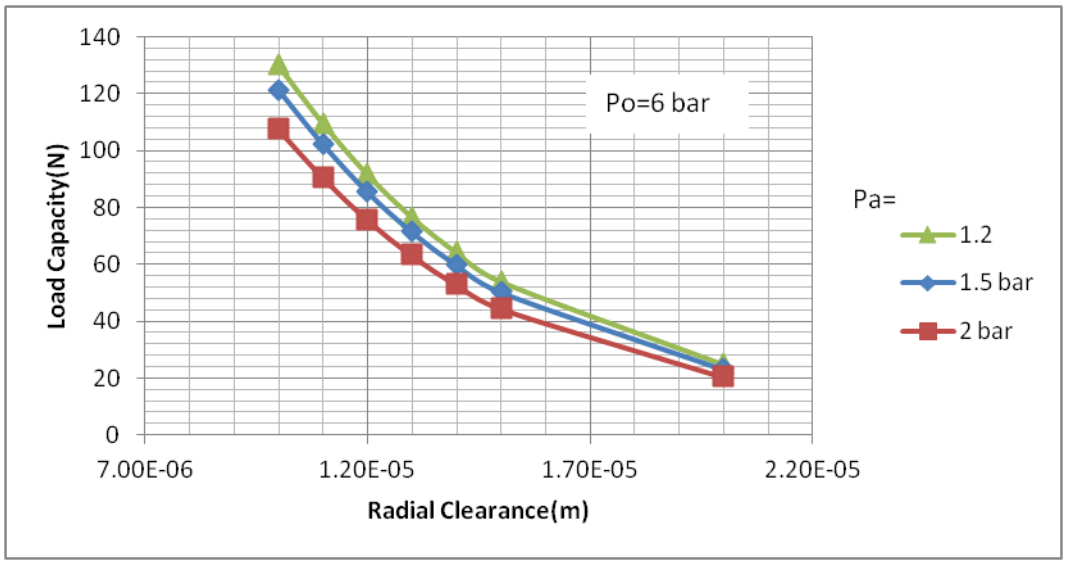

Figure 4.17: Load Capacity Vs Stiffness for different outlet pressures

Here, three different values of outlet pressure have been considered with a constant supply pressure. From the analysis, it was found that increase in outlet pressure results a lower load capacity which is shown in the Figure 4.17.

4.3 Dynamic Analysis of the shaft

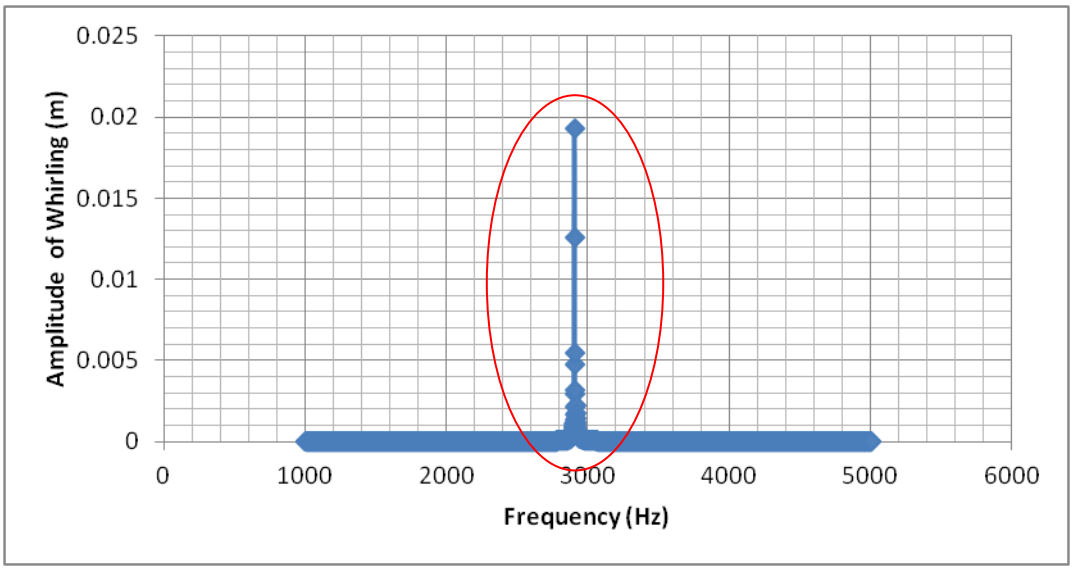

Figure 4.18: Amplitude of whirling without damping Vs frequency

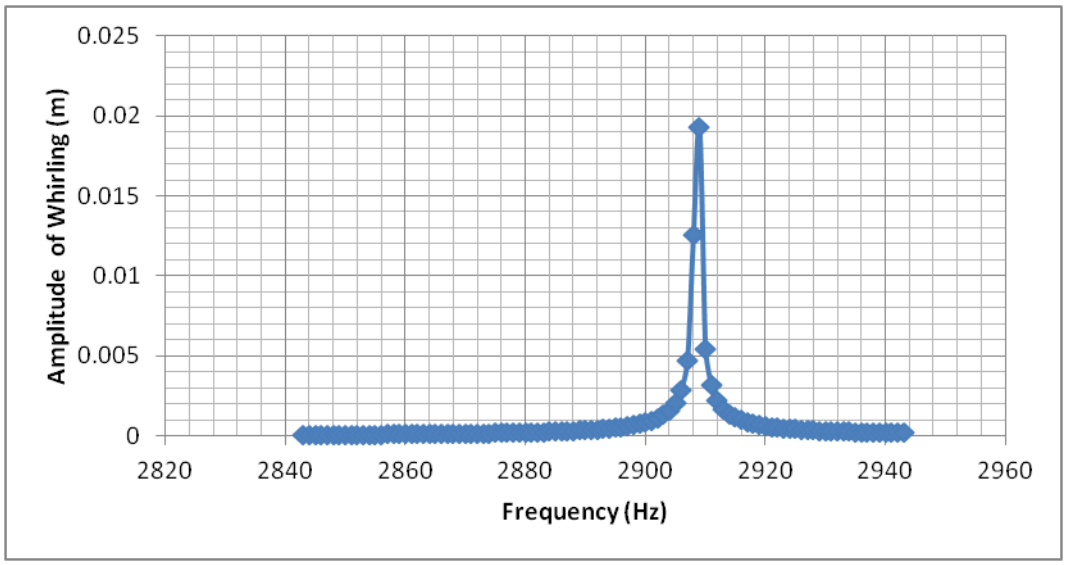

Figure 4.19: Magnification of Figure 4.18

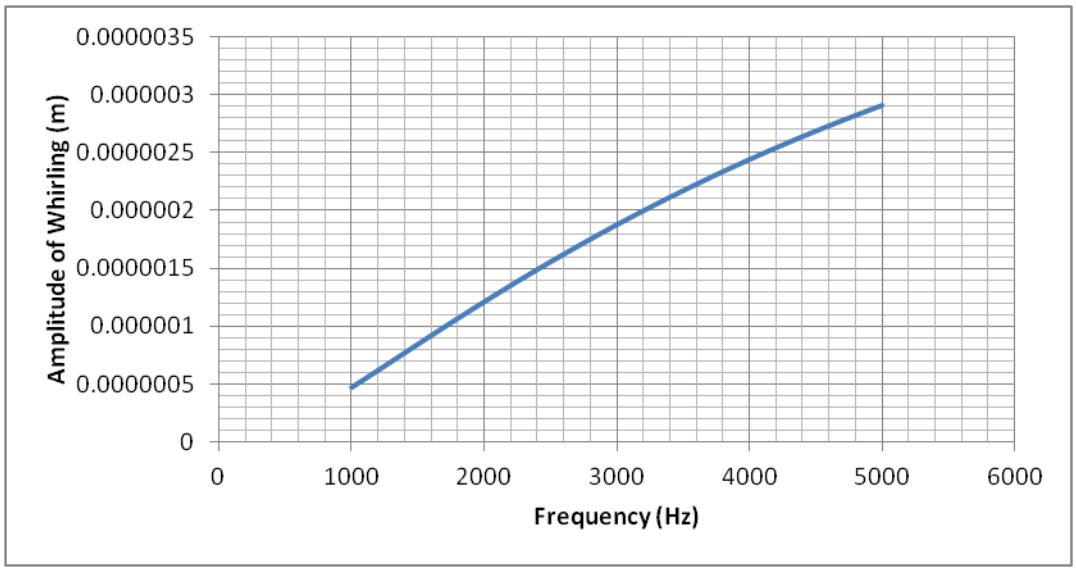

Figure 4.20: Amplitude of whirling with damping Vs frequency

At the lower natural frequency, the amplitude of whirling without damping is found to be 0.019333085 m, whereas with damping it is 1.81726E-06 m. And at higher natural frequency the amplitude of whirling without damping is 4.70164E-05 m and with damping its value is 1.92622E-06 m. At a frequency of 5000 Hz, the amplitude of whirling is 2.90646E-06 m. So our design is safe in the range of 1000-5000 Hz, as the minimum value of clearance is 5.25E-06 m. Though the critical speed is more than 8000Hz, it is better to operate at a lower speed range 1000-5000 Hz.

5 VALIDATION OF ANALYSIS USING ANSYS CFX

5.1 Journal Bearing

For analysis of the fluid flow in the journal bearing, an ANSYS CFX model has been made. As the number of elements with good skewness value for the CFX analysis of very thin fluid layer is very high, so it requires high capacity workstation. So according to the availability of workstation available at IPR, 50µm radial clearance has been taken for the analysis using ANSYS CFX.

Here, the supply port is taken as inlet and the clearance side open to atmosphere is taken as outlet. Inlet is considered as mass flow inlet and the outlet as static pressure outlet.

Table 5.1: Theoretical data considered for the analysis of journal bearing

d_o (m)	d_R (m)	h (m)	b (m)	n	P_o (Pa)	P_a (Pa)	C_d
0.0001	0.001	5E-05	0.0001	16	1200000	120000	0.8

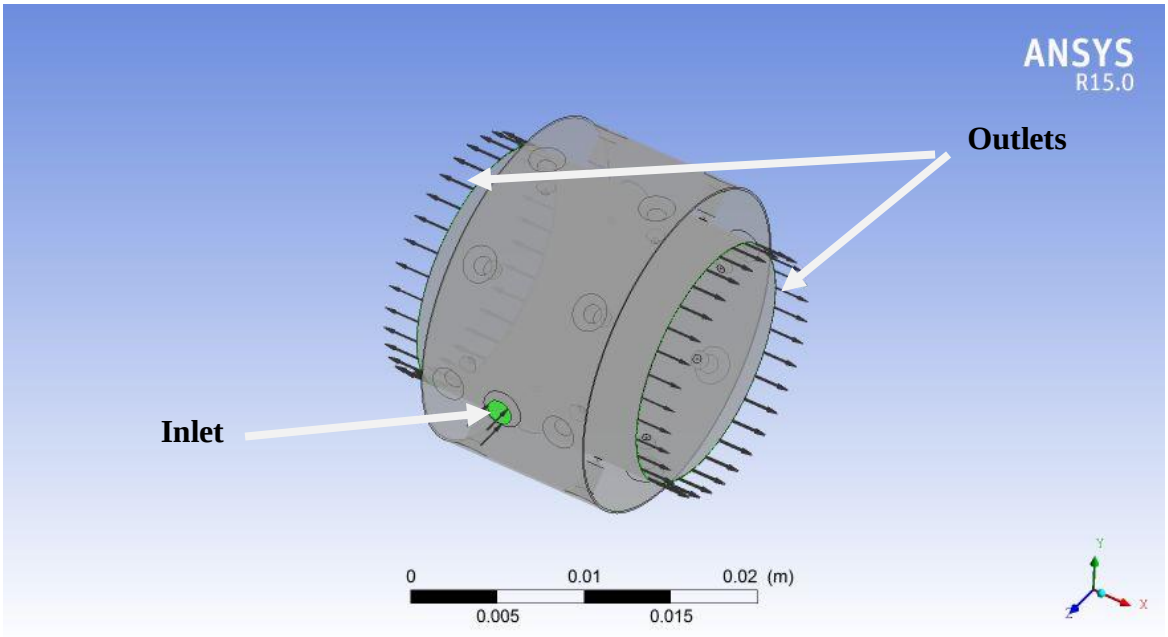

Figure 5.1: Inlet and Outlet of the flow model of journal bearing

Figure 5.1 shows the inlet and outlet of the model as well as the absolute pressure contour of the fluid flow region. From the Figure 5.1 and 5.2, it can be observed that the fluid expands only after the restrictor of the feedhole. So the fluid region before the restrictor is like

reservoir. Figure 5.2 shows the clear variation of pressure on the high clearance and low clearance side. And some low pressure area was found in the pocket of the feedhole region due to high velocity of gas. This high velocity region is shown in the Figure 5.7.

In order to analyze the fluid flow through the feedhole, a plane is sliced as shown in Figure 5.3.

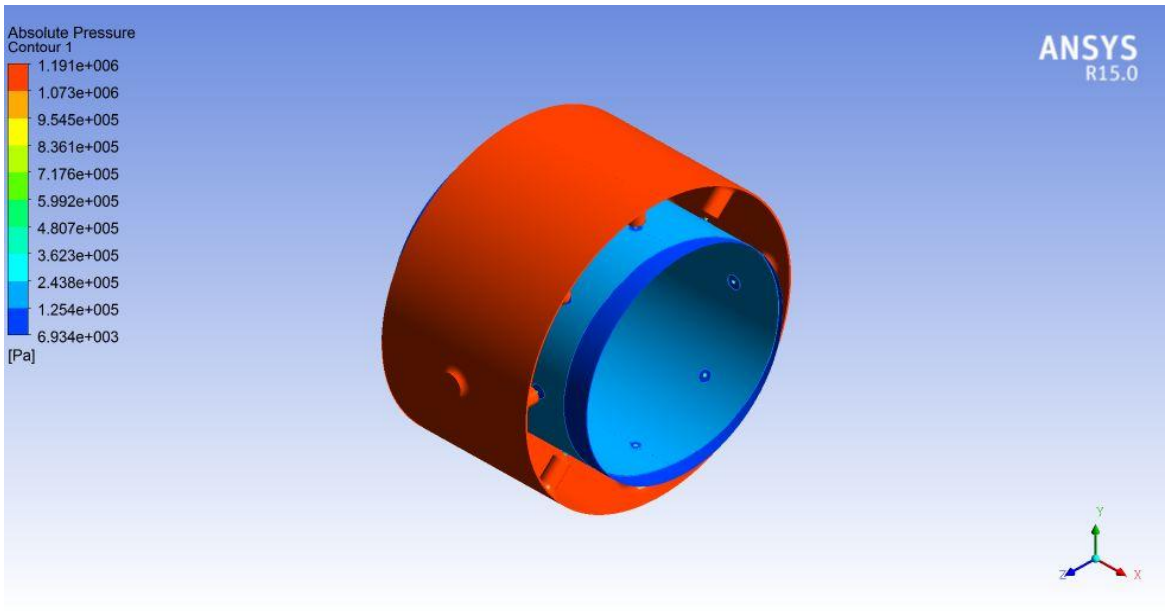

Figure 5.2: Absolute pressure contour of the fluid flow region

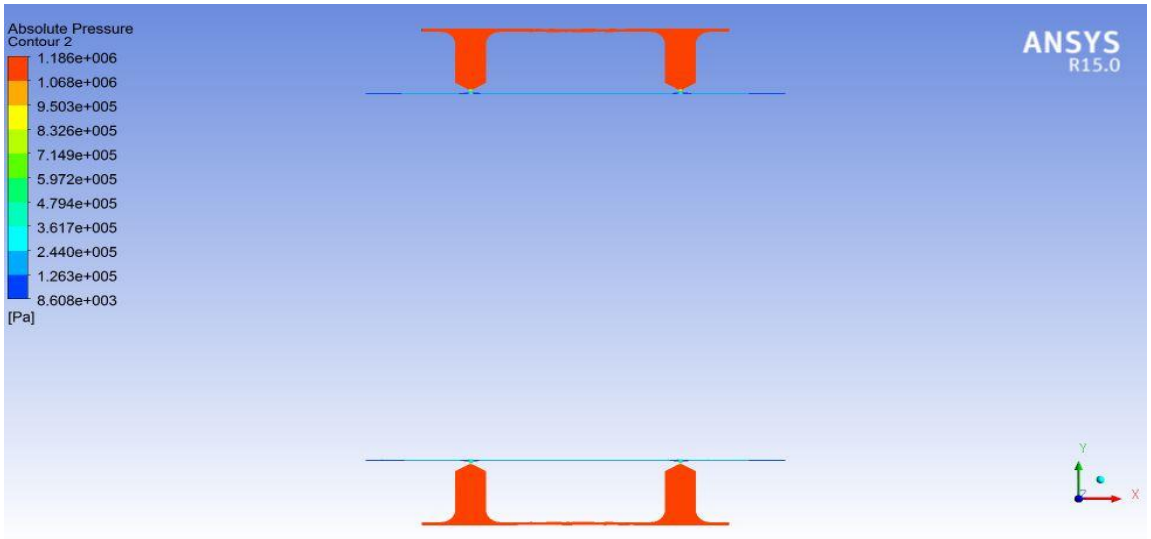

Figure 5.3: Sliced plane view

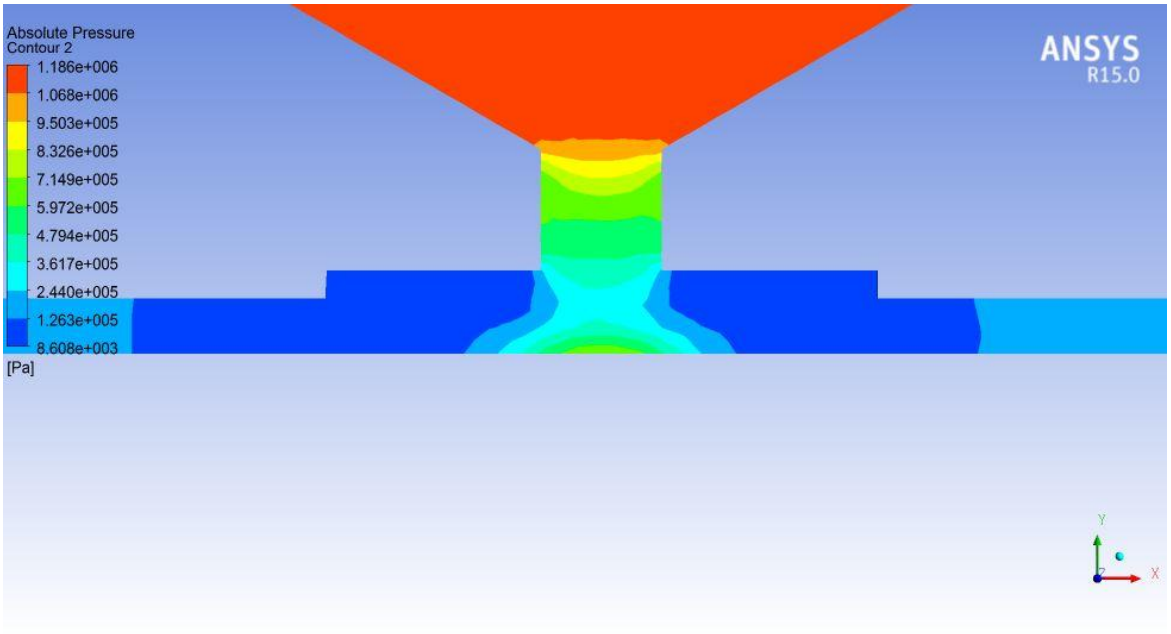

Figure 5.4: Absolute pressure contour of the feedhole region

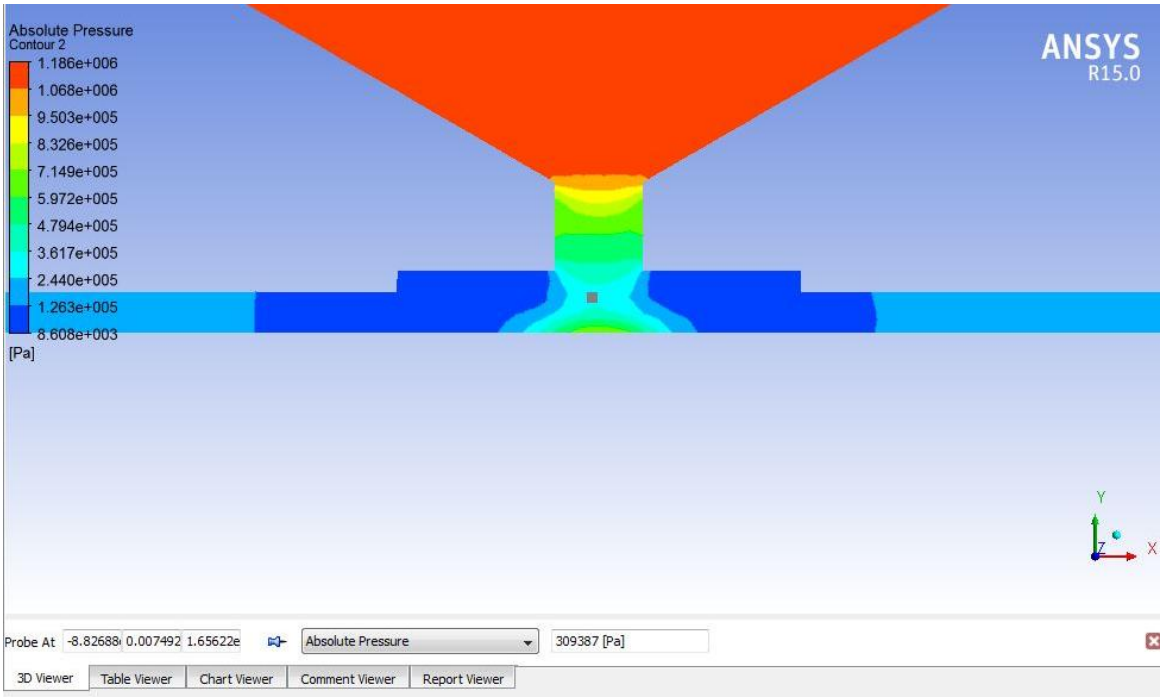

Figure 5.5: Absolute pressure contour of the feedhole region

Figure 5.4 shows the pressure variation at the feedhole region. The gas expands when it come out of the throat of the orifice. But at the downstream of the throat of the orifice, pressure

increases as the velocity of the gas decreases. Figure 5.5 and 5.6 shows the absolute pressure contour of the feedhole region at top and bottom positions respectively. The absolute pressure at the throat at top is nearly 3.09 bar whereas that at bottom, it is 3.26 bar.

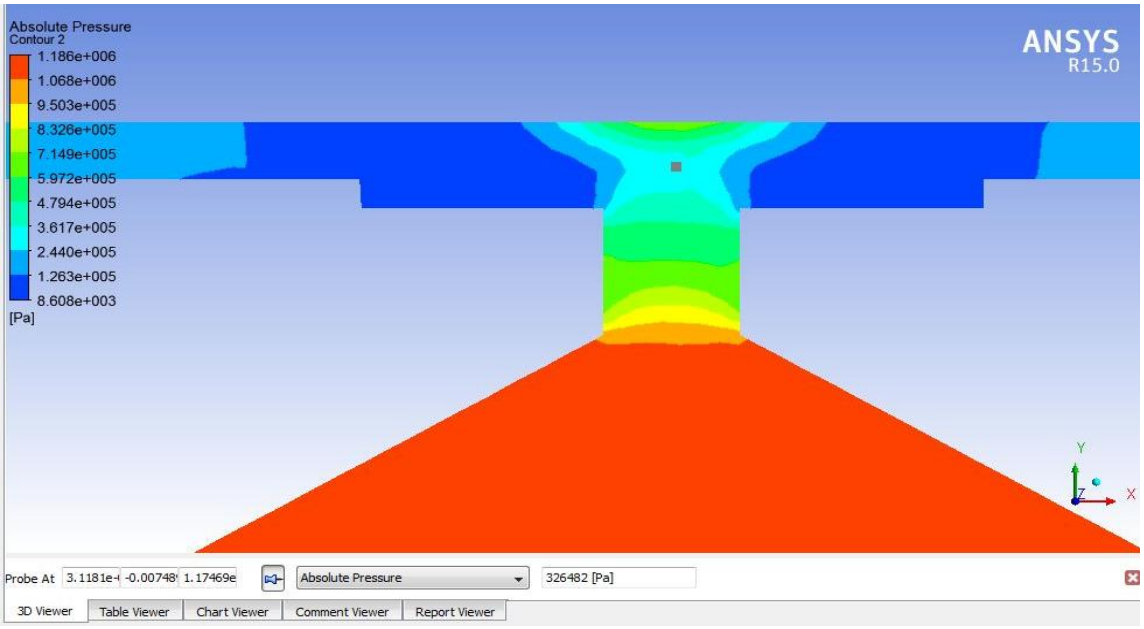

Figure 5.6: Absolute pressure contour of the feedhole region

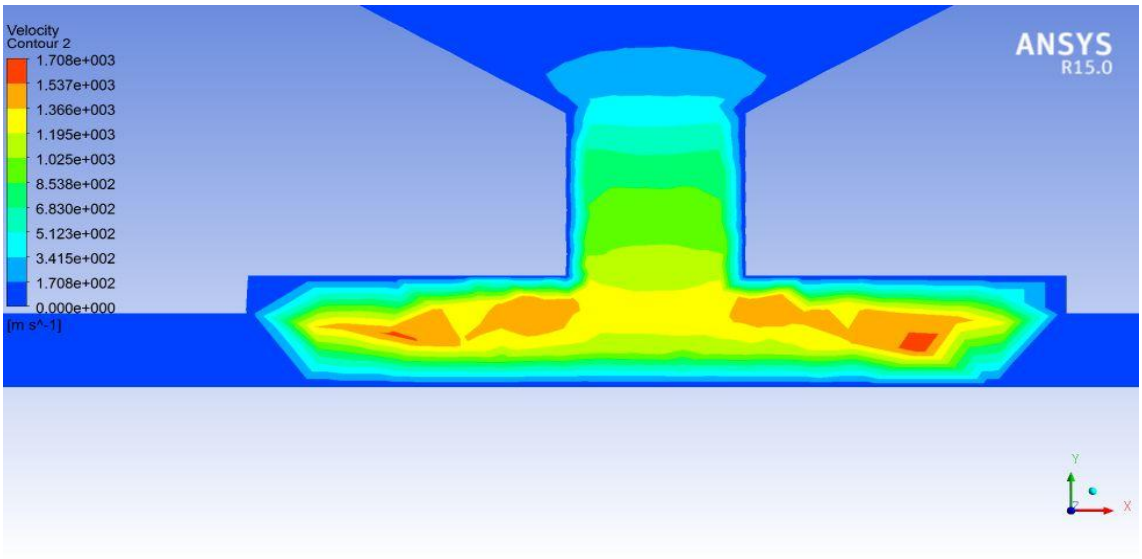

Figure 5.7: velocity contour of the feedhole region

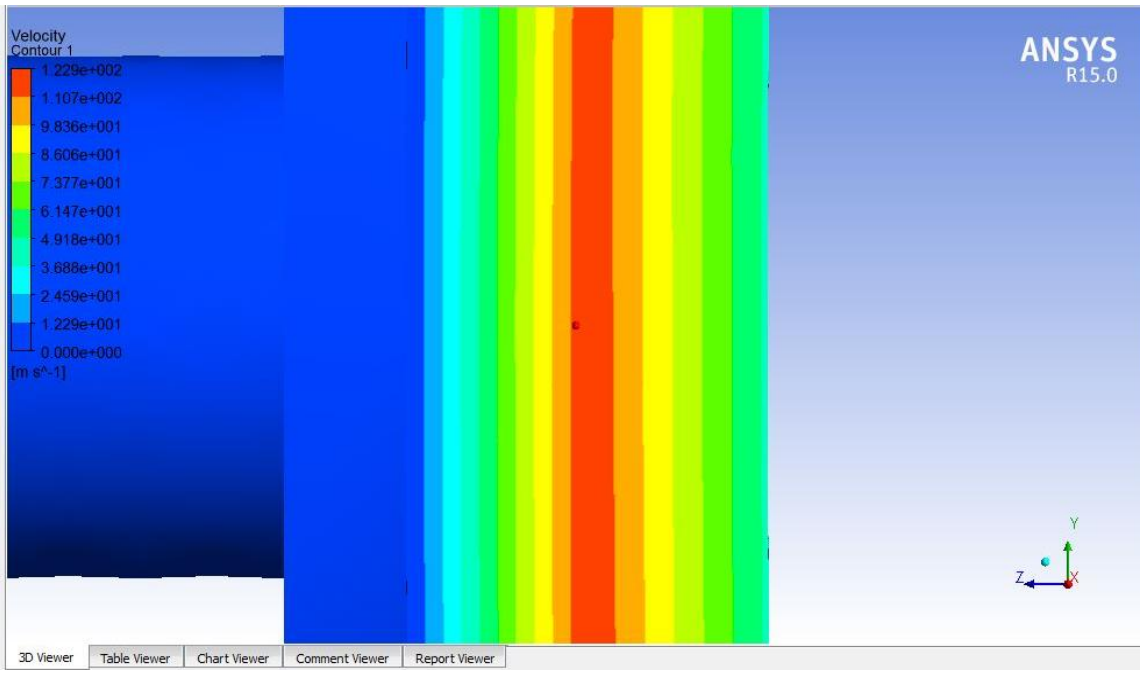

Figure 5.8: velocity contour at 1000 Hz

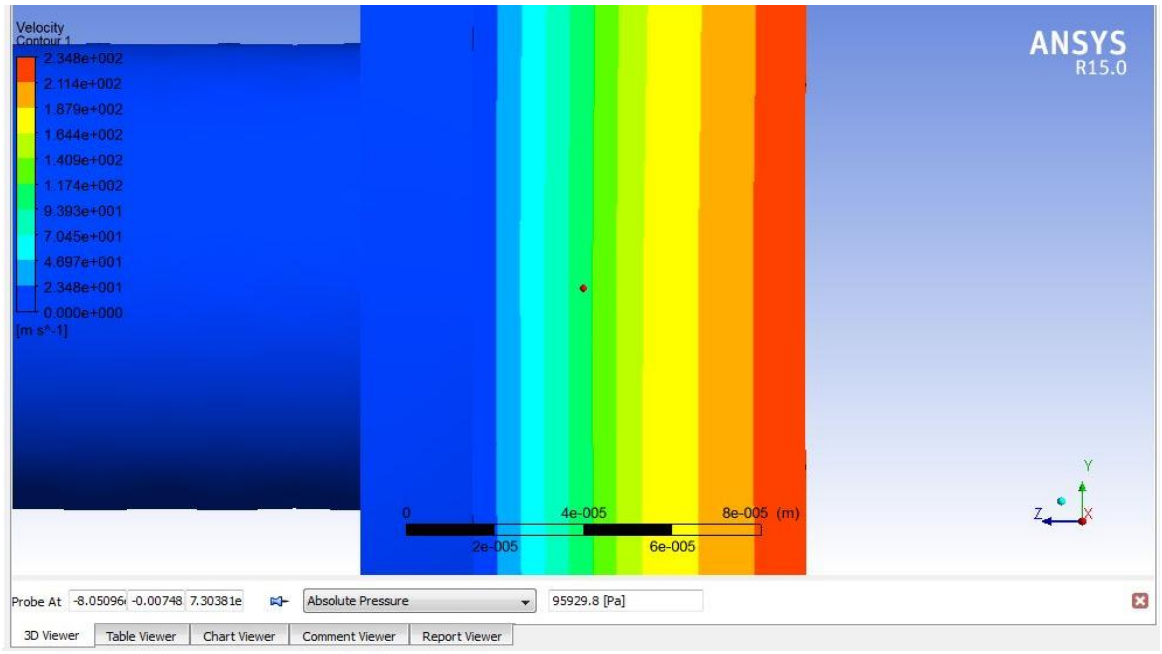

Figure 5.9: velocity contour at 5000 Hz

Table 5.2: Change in pressure at throat of the orifice with change in rotational speed

Speed (Hz)	0	1000	5000
Pressure at high clearance side (Pa)	309387	317821	322365
Pressure at low clearance side (Pa)	326482	330560	334660

Table 5.2 shows that the pressure at the throat of the orifice increases with increase in rotational speed of the shaft. The inlet and the outlet pressure remain the same irrespective of the rotational speed of the shaft. Only the pressure distribution changes across the fluid flow region.

5.2 Thrust Bearing

Similar approach has been made for the analysis of thrust bearing.

Table 5.3: Theoretical data considered for the analysis of thrust bearing

d_o (m)	d_R (m)	h (m)	b (m)	n	P_o (Pa)	P_a (Pa)	C_d
0.00011	0.0009	5E-05	0.00016	12	433700	120000	0.8

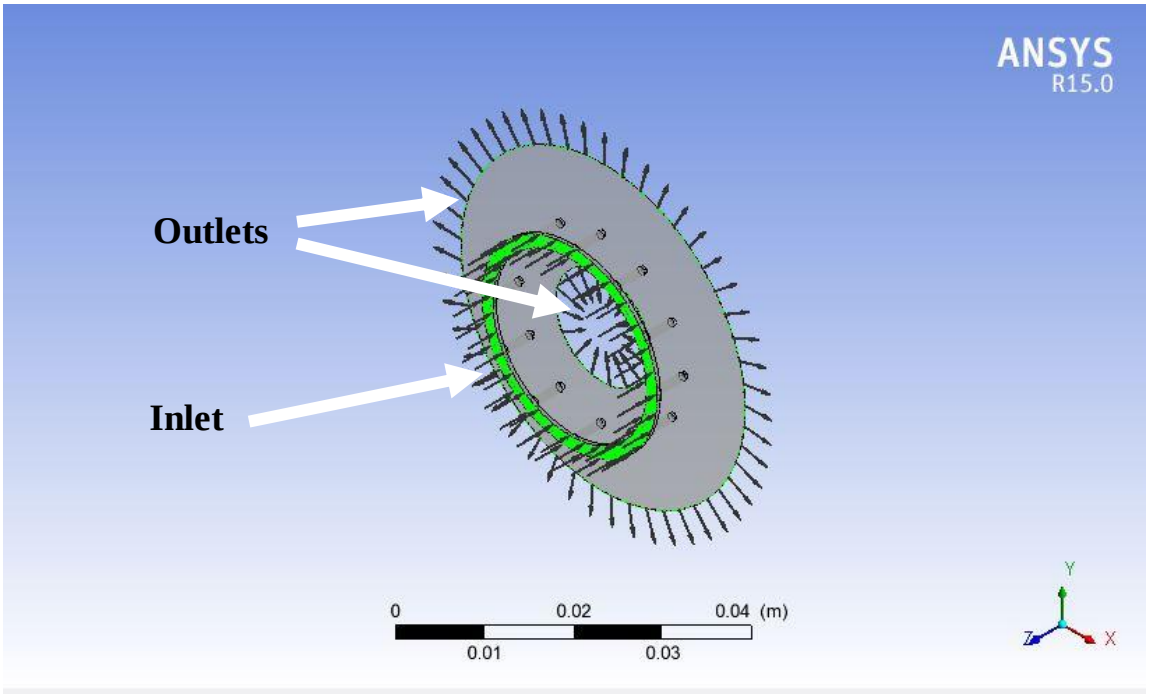

Figure 5.10: Inlet and Outlet of the flow model of thrust bearing

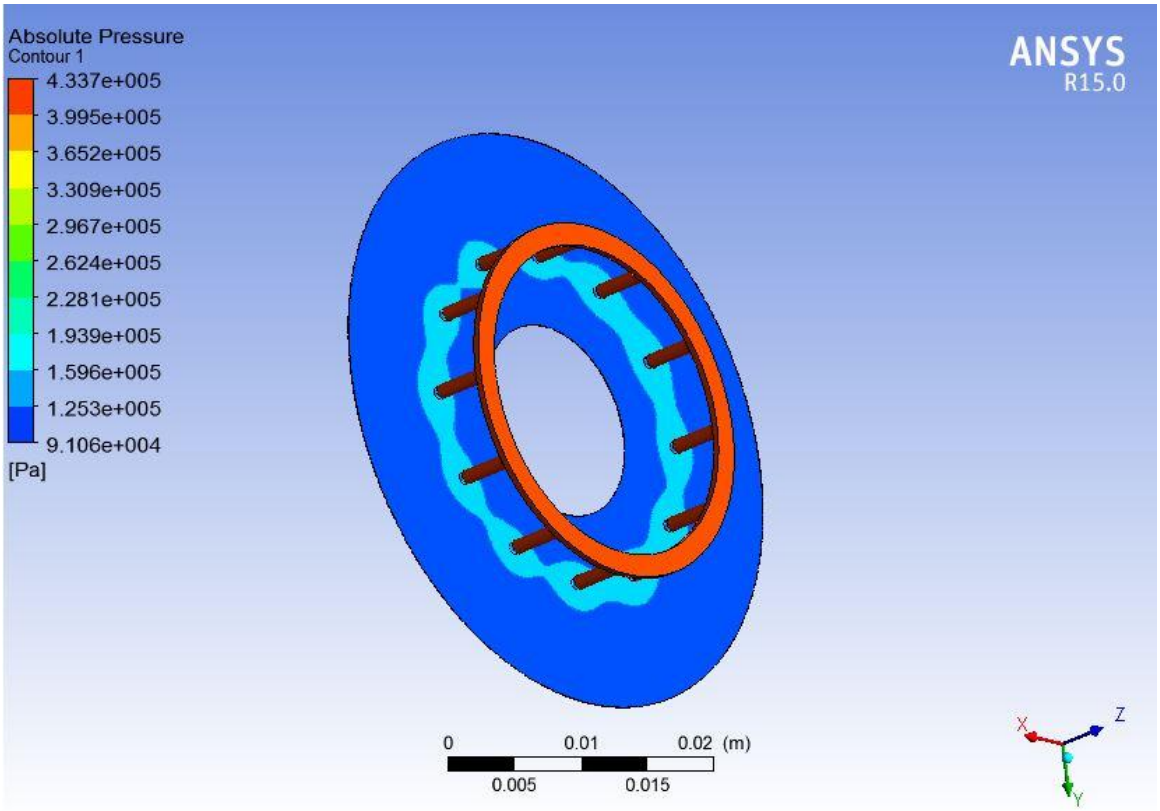

Figure 5.11: Absolute pressure contour of thrust bearing

6 MATERIAL SELECTION

Material selection is the most important thing apart from the design of bearings. While choosing the material, the following properties of the material should have to be considered.

- Materials with low friction and anti-seized properties
- Stress relieved material
- Corrosion resistance
- Thermal expansion
- Machinibility
- Thermal conductivity

Materials having low friction and anti-seized properties help the material for a longer life span. Stress relieved materials are generally stable in nature i.e. in case of stress relieved material, the risk of dimension change is very less. As here fluid is being used as lubricant, so the material should be corrosion resistant for that fluid. The thermal expansion of the material should have to be very less. As feedholes are drilled, so the material should have good machinibility in order to get précised geometry. As the shaft rotates at very high speed, so some amount of heat will be generated in the bearing clearance. For that, the material having good thermal conductivity has to be chosen.

In case of shaft, the material should be light as much as possible and corrosion resistant. Here, SS-410 has been taken as shaft material for the calculation.

7 CONCLUSION

- A simple procedure has been established for the design of the aerostatic hybrid journal bearing, thrust bearing as well as dynamic unbalance of the shaft.
- For the design of the journal bearing, we should go for low mass flow rate i.e. low clearance and low orifice diameter in order to get high stiffness. Before going for design, we should set the target value of the stiffness, so that we can optimize our design parameters.
- By increasing the inlet pressure, high stiffness value can also be obtained.
- The dynamic analysis is done for a certain stiffness value of the bearing. Here, the amplitude of the whirling of shaft with damping, at the two natural frequencies found within our safe limit. For this case, the value of critical frequency for self induced vibration is three times of the lower natural frequency, more than 8000 Hz. But for safety, we should go for lower range of operating frequency. In this study, dynamic analysis for the range 1000-5000 Hz has been done and found safe in that range.
- The lower natural frequency can be shifted to a higher value with increase in aerostatic stiffness of the journal bearing.
- As amplitude of vibration increases with increase in rotational speed of the shaft, so vibration can be reduced by decreasing the rotational speed of the shaft.
- In the ANSYS CFX analysis, for the mass flow rate of 0.123g/s, the outlet pressure is found 11.9 bar, which is nearer to our theoretical value of inlet pressure 12 bar. The mass flow rate in ANSYS CFX analysis is 13 % more than that of theoretical calculation.
- In case of thrust bearing, at 4.337 bar inlet pressure, the mass flow rate is found to be 0.0465 g/s for using ANSYS CFX, which is 38 % more than the theoretical value.
- For the future work, dynamic analysis of the thrust bearing, system coupling analysis of bearing for load calculation by using ANSYS can be done.

8 REFERENCES

1. Powell, J.W. Design of Aerostatic Bearings. Machinery Publishing, 1971.

2. Pink, E. G. and K. J. Stout. "Design procedures for orifice compensated gas journal bearings based on experimental data." *Tribology International* (1978): 63-75.

3. Robinson, C. H. and F. Sperry. *The static strength of pressure fed gas journal bearings*. A.E.R.E. Report R2462. United Kingdom, 1958.

4. Shires, G. L. and D. Pantall. "The aerostatic jacking of a vented aerodynamic journal bearing." *Institution of Mechanical Engineers* Lubrication and Wear Group Convention (1963).

5. Dudgeon, E. G. and I. R. G. Lowe. "A theoretical analysis of hydrostatic gas journal bearings." Canadian NRC Report MT54. 1965.

6. Wilcoek, D. F. "Design of Gas Bearings." *Mechanical Technology Incorporated* (1967).

7. Constantineseu, V. N. "An approximate method for the analysis of externally pressurised gas journal bearings." *Gas Bearing Symposium*. University of Southampton, 1967.

8. Pink, E. G. "Investigations into design methods for externally pressurized gas journal bearings." *Tribology International* (1974): 265-269.

9. Lund, J. W. "The Hydrostatic Gas Journal Bearing With Journal Rotation and Vibration." *Journal of Basis Engineering* 86.Series D (1964): 328-336.

10. Lund, J. W. "A Theoretical Analysis of Whirl Instability and Pneumatic Hammer for a Rigid Rotor in Pressurized Gas Journal Bearings." *Trans. ASME* (1967): 154-165

11. Raimondi, A. A. "A Numerical Solution for the Gas Lubricated Full Journal Bearing of Finite Length." 4.1 (1961): 131-155..

12. Choudhury, B. K. Design and Construction of Turboexpander based Nitrogen Liquefier. Phd Thesis, National Institute of Technology, Rourkela, 2013.

13. https://webbook.nist.gov/chemistry/fluid

14. Pande, S. S. "Analysis of tapered land aerostatic bearings for combined radial and thrust loads (yate's cofiguartion)." *Wear* 107 (1986): 299-315.